UNIVERSITY OF OKLAHOMA

GRADUATE COLLEGE

TARGET TRACKING USING WIRELESS SENSOR NETWORKS

A DISSERTATION

SUBMITTED TO THE GRADUATE FACULTY

in partial fulfillment of the requirements for the

Degree of

DOCTOR OF PHILOSOPHY

By

PHUONG PHAM
Norman, Oklahoma
2012

TARGET TRACKING USING WIRELESS SENSOR NETWORKS

A DISSERTATION APPROVED FOR THE
SCHOOL OF ELECTRICAL AND COMPUTER ENGINEERING

BY

Dr. Sesh Commuri, Chair

Dr. Sridhar Radhakrishnan

Dr. Joseph P. Havlicek

Dr. Choon Yik Tang

Dr. Tian-You Yu

To my parents for their constant love.

Acknowledgements

First and foremost, I would like to thank my advisor Dr. Sesh Commuri for the guidance, support, and supervision he has given during my doctoral studies. Without his help, this dissertation would not have been possible. I am always indebted to all the things he has done for me.

I owe my gratitude to Dr. Joseph Havlicek, Dr. Sridhar Radhakrishnan, Dr. Choo Yik Tang, and Dr. Tian Yu. They not only spend time serving in my dissertation committee, but also offer me a lot technical advice. I have also learned many interesting concepts through taking their classes or being their teaching assistant.

I also would like to thank Dr. J.R. Cruz and Dr. Keri Kornelson for teaching me many inspiring lessons.

I would like to thank to my lab mates and my ECE friends for their technical help and for being great friends. I want to single out Anh Mai, Dr. Chuong Nguyen, Dr. Minh Ta, Dr. Fares Beainy, Erika Kolher, Damian Vigouroux, Sree H. Gadigota, Nam T. Nguyen, Hoa Pham, and Nam H. Nguyen.

I would like to acknowledge my friends from Society of Vietnamese Students: Hien Hoang, Hoat Tran, Aunt Ha, late uncle Larry, Nghia Tran, Anh P. Nguyen, Dr. Son Hoang, Dr. Huong Pham, Dr. Linh Do, Dr. Tung Tran, Dr. Phuong Le, Tram Truong, Trung Tran, Hoai Nguyen, Dung Phan, and Duc Tran. I consider them as my family members. Moreover, my close friends Anh Tu Nguyen, Quan H. Luu, Tan X. Le and Hai V. Le deserve a special mention.

Last but not least, I want to show my deepest appreciation to my extended family, I were not the person I am today without the love, support and patience of my late grandparents, my parents, my wife, my daughter, my son, my brothers, my parents-in-law, aunt Huong, uncle Giao, aunt Hong, and uncle Thang.

Table of Contents

Contents

List of Tables

List of Figures

Abstract

Tracking of targets in remote inaccessible areas is an important application of Wireless Sensor Networks (WSNs). The use of wired networks for detecting and tracking of intruders is not feasible in hard-to-reach areas. An alternate approach is the use of WSNs to detect and track targets. Furthermore, the requirements of the tracking problem may not necessarily be known at the time of deployment. However, issues such as low onboard power, lack of established network topology, and the inability to handle node failures have limited the use of WSNs in these applications. In this dissertation, the performance of WSNs in remote surveillance type of applications will be addressed through the development of distributed tracking algorithms. The algorithm will focus on identifying a minimal set of nodes to detect and track targets, estimating target location in the presence of measurement noise and uncertainty, and improving the performance of the WSN through distributed learning.

The selection of a set of sensor nodes to detect and track a target is first studied. Inactive nodes are forced into 'sleeping' mode to conserve power, and activated only when required to sense the target. The relative distance and angle of the target from sensor nodes are used to determine which of the sensors are needed to track the target.

The effect of noisy measurements on the estimation of the position of the target is addressed through the implementation of a Kalman filter. Contrary to centralized Kalman filter implementations reported in the literature, implementation of the distributed Kalman filter is considered in the proposed solution.

Distributed learning is implemented by passing on the knowledge of the target, i.e. the filter state and covariance matrix onto the subsequent node running the filter. The problem is mathematically formulated, and the stability and tracking error of the proposed strategy are rigorously examined. Numerical examples are then used to demonstrate the utility of the proposed technique.

It will be shown by mathematical proofs and numerical simulation in this dissertation that distributed detection and tracking using a limited number of nodes can result in efficient tracking in the presence of measurement noise. Furthermore, minimizing the number of active sensors will reduce communication overhead and power consumption in networks, improve tracking efficiency, and increase the useful life span of WSNs.

Chapter 1

Introduction

1.1 Background on Wireless Sensor Networks

Recent advances in communication technologies and electronic systems have enabled the widespread use of Wireless Sensor Networks (WSNs). A sensor network is an ad hoc network comprising of a large number of sensor nodes that can individually sense their environment and communicate the sensed data to a network sink, typically in a multi-hop fashion. The low cost and small size of sensor nodes have resulted in WSNs being used in a variety of applications such as military, health care, environmental monitoring, structural health monitoring, industrial automation, and remote surveillance. However, WSNs are yet to reach their full potential as their performance is limited by the lack of organization, the constrained onboard power and processing capability, and the issues with routing and communication of the sensed data. To overcome these limitations, researchers have extensively investigated many aspects of WSNs through the development of algorithms for deployment [1-3], coverage [4-7], medium access control (MAC) protocols [8, 9], routing protocols [10, 11], and the use of WSNs in applications [12]. Some of these results are discussed in the following subsections.

1.1.1 Deployment and Coverage

The key issues to be addressed during the deployment of WSNs are the abilities of the network to sense parameters of interest in a given region and to transmit the sensed data to users outside the network. Given a geographic area, the problem is to find an optimal deployment strategy that minimizes the number of required sensors to meet the sensing criterion. In environments that are easy to access, sensor nodes can be deployed in a deterministic manner [13, 14]. Placement of sensor nodes at the vertices of a hexagonal lattice is known to provide optimum coverage of a two-dimensional region. Similarly, placement of sensor nodes at the vertices of a face-centered cubic lattice is known to provide optimum coverage of a three-dimensional region [15]. However, it is infeasible and impractical to archive deterministic deployment in inaccessible or hazardous areas. Deployment of WSNs in such inaccessible regions is usually performed in a random manner. Consequently, the determination of the extent and type of coverage are the issues to be examined during the deployment of sensor networks [16, 17]. Several applications also require the coverage of every location in the sensed region by multiple sensor nodes. This problem is usually formulated as a k-cover problem where each location is covered by at least ‘k’ sensor nodes [6].

Several researchers have investigated coverage issues in WSNs [18]. Li [4] developed an algorithm for optimum best-coverage-path with the least energy consumption. The problem of sensor placement and border perambulation have been investigated by Watfa and Commuri in [1, 7]. Solution to the energy-efficient coverage problem was also investigated by Cardei in [19].

While existing results in the literature address several key issues in the deployment of WSNs and their region of coverage, requirements of specific node distribution or coverage by multiple nodes have to be addressed prior to their use in target tracking applications. The use of multiple sensor nodes to track a dynamic target increases the risk of bottlenecks in communication of the target information. This could also result in rapid depletion of onboard power and early failure of the sensor nodes.

1.1.2 Medium Access Control (MAC) Protocols

Since sensor nodes share the wireless medium, MAC [9] protocols are required to operate a sensor network, to utilize the shared wireless spectrum by all the nodes in the network. Additional, these protocols schedule the transmissions by individual nodes, to avoid collision between data packets in the network. Issues such as fairness, throughput, latency, energy efficiency, and bandwidth utilization in WSNs can be also addressed through MAC protocols [9, 20].

Energy utilization in a WSN is usually investigated by forcing individual nodes into the 'sleeping' mode, when the nodes consume the least amount of energy. Nodes are 'woken' up periodically to 'sense and report' before being forced back into the sleeping mode. Since these nodes function in an ad-hoc manner, they need to contend for the wireless channel before transmitting any data. Contention-based MAC protocols [20, 21] minimize the simultaneous transmissions of data packets by more than one node, and avoid collision of data packets. Thus, individual nodes can effectively use available onboard power. MAC protocols, which schedule individual nodes to transmit data sequentially, perform better than Time Division Multiple Access (TDMA) techniques.

Contention for wireless resource among sensor nodes can also be resolved through reservation mechanisms or scheduling mechanisms. In reservation mechanisms, a node is reserved a time slot for sending data. In contrast, a node is scheduled to send data in a specific time slot in scheduling mechanisms [22]. Energy consumption in a WSN was also studied through Sensor-MAC (SMAC) protocol [23] where synchronization and periodic sleep-listen schedules were managed locally by each node. Some researchers [22-26] proposed dynamic low duty cycle or increased inactive time of sensor nodes to manage power consumption in a WSN. Unfortunately, such techniques can result in lower overall performance of the WSN. In an attempt to further conserve power and improve performance, Pattern-MAC (PMAC) [27] was proposed to address the changes in duty cycle time of sensor nodes depending on the traffic pattern in the network.

Most of the available protocols implemented the same active and inactive pattern for all sensor nodes, which is not efficient for the target tracking application. When a target is in the proximity of sensor nodes, these nodes need to be active all the time and be ready to take measurements. In contrast, the sensor nodes can set their duty cycle much lower if a target moves out of their sensing range. This issue needs to be examined for the successful use of WSN in target tracking applications.

1.1.3 Routing Protocols

The main goal of routing protocols in WSNs [28] is to deliver accurately and timely sensed data from sensor nodes to the network sink. Important characteristics of routing protocols are energy efficiency, scalability, and adaptability to changes in the network. Energy efficiency probably plays the most important role of routing protocols as it determines the life span of WSNs.

Routing protocols can be categorized in terms of network structure as flat, hierarchical, or location-based. In flat routing, every node has the same role, while in hierarchical protocols cluster head nodes aggregate data from their neighbor nodes, process the collected data, and transmit the processed data to the network sink. Flat routing techniques are extensively studied in works such as 'Sensor Protocols for Information via Negotiation' (SPIN) [29], 'Sequential Assignment Routing' (SAR) [30], direct diffusion protocol [31], among others. 'Low Energy Adaptive Clustering Hierarchy' (LEACH) [32] and 'PEGASIS: Power-Efficient Gathering in Sensor Information Systems' [33] are typical examples of hierarchical protocols. In location-based protocols [34, 35], routing paths are computed depending on the network structure and the locations of sensor nodes.

Routing protocols also can be categorized according to their operation as multipath-based, query-based, QoS-based, and coherent-based [36, 37]. Routing protocols can be classified through the nature of their operation as: proactive, reactive, or hybrid [20]. In proactive or table-driven protocols [38, 39], all routes are computed in advance. Thus, when a sensor node has to transmit data, it can send the data immediately without any delay. However, such an approach is not desirable as it requires significant amount of energy to compute all routing paths in advance. Moreover, these routing paths may not be available as sensor nodes fail due to depletion of power. In reactive or 'on demand' protocols [39, 40], routes are computed at the time of transmission. In comparison to their proactive counterparts, reactive protocols are more energy efficient, but subject to higher latency in transmission due to route calculation. A balance between these two approaches is achieved in hybrid protocols [41, 42] where a combination of proactive and reactive protocols are used depending on the nature of transmission. One approach to reduce the number of data packets transmitted in the network, thus reducing total power consumption, is to aggregate data from several sources before transmitting it to a network sink. Another method is to process the raw data and report only the information contained therein.

While routing protocols in the literature adequately address the majority of issues in WSNs, further research is needed prior to their use in target tracking. When there is no target present in the network, only the sensor nodes on the border of the surveillance region need to be active, and all the nodes inside the region can be placed in a 'sleeping' mode. If the target is within the range of the WSN, all the nodes that actively track the target must be in full operational mode. Additionally, the quality of service of the transmission route from the sensor nodes to the network sink must be guaranteed.

1.1.4 Applications

In recent years, WSNs have been used in a variety of applications including health care [43], structural health monitoring [44], military applications [45], environment monitoring [46], surveillance, and security applications. WNSs are also used in commercial applications such as inventory management and industrial process control. Since each application has its unique characteristics and requirements, no single protocol can be suited for all applications. Since most of the MAC and routing protocols in WSNs are designed for low-data rate applications, additional research is needed prior to their use in target tracking type of applications that typically involve sporadic but high rate of communication.

Target tracking using WSNs has been u

1.2 Target Tracking in Wireless Sensor Networks

Tracking targets in remote inaccessible areas has emerged as one of the important applications of WSNs [47]. The goal of the tracking algorithm is to determine the position of target with minimum error. To meet this goal, the location of the target has to be determined. Consequently, estimation techniques can be used to minimize the tracking error. Moreover, an autonomous vehicle can be used in conjunction with static sensor nodes to increase both the computational capability and reliability of the tracking algorithm. Finally, extending the useful life of the sensor network is one of the primary goals for the tracking system.

1.2.1 Localizing Methods

There are several approaches to the problem of detecting the location of a target from disparate sensor measurements. Trilateration is a popular approach when the range of the target from each sensor node is known. Triangulation [48, 49] on the other hand, is the preferred method when only the bearing of the target from the sensor node is known. For example, common trilateration techniques use Global Positioning System (GPS) [50], Received Signal Strength (RSS), or Time of Arrival (TOA) to localize [51-55] targets. Triangulation, on the other hand, uses techniques such as Angle of Arrival (AOA) [49] to estimate the location of the target .

Trilateration is an algorithm for estimating the coordinates of an object given its distances from known locations. This process is straightforward if the range measurements are error free. However, in practice, the uncertainty in range measurements and the spatial distribution of reference locations affect the accuracy of the algorithm. A number of methods have been proposed to improve the performance of trilateration algorithm. Groginsky [56] proposed a recursive formula to analyze the effect of spatial distribution of referenced locations and range measurement error on the accuracy of the calculated position. Fang [51] proposed a closed-form approach to estimate the position of an object and the time of its measurement using GPS data. Manolakis [44] derived formulae for the joint variance and bias of the position estimates based on special distribution of reference points and uncertainty in the range measurements. Recently, Thomas and Ros [54] used the Cayley-Menger determinant to derive the trilateration error in the presence of both measurement errors and station location errors.

The error resulting from trilateration algorithm is the combination of the joint distribution of range measurement errors and station location errors. The uncertainty of the error has to be bounded if further estimation techniques are used to minimize the error in measurement. However, the uncertainty in measurements is not necessarily bounded in randomly deployed WSNs. Therefore, conditions under which this uncertainty is bounded have to be determined.

Triangulation is a method for determining the location of an object by the angular measurements from two known locations. Triangulation method has been widely used in military applications such as missile guidance, air defense, as well as in civilian applications. Pieper et al., [57] proposed a dual-based line algorithm using passive sensors to address the relationship between the tracking range and the precision of triangulation algorithm. Shams [58] used an artificial neural network to determine the optimal triangulation algorithm for target localization. The determination of the location of a sensor node in a random deployment can also be addressed using triangulation algorithm [59]. The accuracy of the triangulation algorithm depends on several factors including the error in angular measurements, the distance between the reference locations, and the location of the target.

1.2.2 Estimation Techniques for Target Tracking

While localization techniques can be used to determine the location of the target, the accuracy of the measurement is affected by the range measurement error as well as the errors caused by spatial distribution of sensor nodes. Estimation techniques can be used to reduce the effect of these errors on the estimated position of the target. The Kalman filter [60], which requires the state of the system be linear and the distribution of measurement noise be Gaussian, is one of the most well-known techniques for estimation. Particle filters offer an alternative technique for estimating the location of the target when the distribution of measurements is not Gaussian and/or the state of the system is nonlinear.

1.2.3 Kalman Filters

Since its introduction in 1960, the Kalman filter [60] has been one of the most popular estimation techniques, especially for the tracking type of applications. Under the assumptions of linearity in the system dynamics and Gaussian distribution of measurement noise, the Kalman filter can be shown to result in the minimum variance of the estimation error [61]. However, since most of the practical systems are nonlinear, the Extended Kalman filter (EKF) was proposed to address the nonlinearity in the system dynamics. The EKF guarantees the stability and convergence of estimated errors

[62, 63] provided that the system meets some specific conditions. Otherwise, the estimated errors of the EKF can diverge [64, 65].

Recently, Kalman filters have been proposed to overcome the effects of measurement noise and uncertainties in WSNs in target tracking applications [66-72]. Two classes of Kalman filter-based approaches have been implemented in WSNs.The first approach is a centralized implementation of the Kalman filter [72] where every sensor node takes measurements and sends the measured data to a centralized node which runs the filter. In this approach, the power of the sensor node will be depleted quickly because of excessive measurements and inter-node communication. Moreover, it is impractical for all sensor nodes to communicate with a centralized node due to limitations in communication range.

In the decentralized approach, only a finite set of sensor nodes within the proximity of the target take measurements and communicate the measured data to other nodes. The Kalman filter is implemented locally on one node in each sensing region. This method is scalable and can be applied effectively in WSNs. Decentralized, as well as distributed Kalman filters were investigated by Olfati-Saber [70, 71] and by Cattivelli et al., in [66]. Distributed Kalman filters in these approaches implement distributed processing of the estimation algorithm wherein each node runs its own version of Kalman filter and shares the learned information with other neighbor nodes in order to reach a consensus value of the estimate. The number of neighbor nodes determines the cost of the algorithm in terms of power consumption and communication complexity. Consequently, these approaches are not efficient for target tracking problems as they require extensive inter-communication among neighbor nodes.

1.2.4 Particle Filters

Practical tracking systems are not necessarily linear, and the noise distribution is non-Gaussian. Recently, particle filters [73, 74], also known as Sequential Monte Carlo methods (SMC), have been used in WSN to track targets [75-77]. These techniques are power intensive and require significant amounts of onboard power for communication and computation thereby resulting in shorter life span of the sensor network. Moreover, it is challenging to choose the right number of particles used in SMC methods, as this parameter can affect the convergence properties of the particle filter. On the other hand, in a dense sensor network it is feasible to select a set of sensor nodes in the neighborhood of the target, thereby guaranteeing bounded uncertainty in the joint measurement. However, Kalman filters are still preferred for achieving desired trade-off between energy consumption in the network and the reduction of tracking errors.

1.2.5 Mobile Robot Assisted Target Tracking

The use of mobile robots in surveillance, perimeter patrol, and target tracking applications has also been widely studied [78]. Motion planning of nonholonomic mobile robot was first presented [79, 80]. Coordinated control of mobile robots was studied by Jung and Sukhatme in [81]. However, determining the location of a target using one mobile node is not an easy task. The use of mobile robots in conjunction with WSNs can address this problem. Moreover, due to mobile robots' higher computational capacity in comparison with that of statistic sensor nodes and their ability to move in the sensor field, the tracking quality is improved greatly.

1.2.6 Energy Efficiency

Energy efficiency and extending the useful life of the WSN are some of the other major challenges. In order to save energy, a sensor node should be put in the sleep mode for the majority of the time either by reducing its duty cycle or through smart scheduling. However, in the target tracking application, a set of sensor nodes is required to be active when the target moves to its proximity. Thus, the first challenge to be discussed is the selection of a set of sensors [82, 83] within the measurement range of the target, that results in the smallest bias in estimation. Due to the effect of geometric dilution of precision [84, 85], increasing the number of sensors used for tracking does not always result in improving the accuracy of the estimates.

Kalandros and Pao [86] proposed a covariance control method for selecting a group of sensor nodes satisfying a given error covariance matrix. On the other hand, Atia et al., [87] used partially observable Markov decision process to schedule sensor nodes that optimized the trade-off between tracking performance and energy consumption. Once sensed nodes are determined, then the second challenge is to determine the trilateration uncertainty. Extending the life time of WSNs by reducing the overall power consumption is another challenge that has to be investigated [31, 88]. Generally, the sensor nodes that have more residual power are preferred over nodes with less residual power for use in tracking and sensing applications. Furthermore, in a tracking system using range measurement sensors, it should be ascertained that the selected sensor nodes satisfy the constraint on trilateration uncertainty.

1.3 Scope of the Dissertation

The challenge of acquiring and tracking a dynamic target using WSNs is addressed in this research. Issues specific to deployment, coverage, scheduling of the sensor nodes, as well as target acquisition and location will be studied and their impact on the tracking accuracy will be analyzed. Throughout the dissertation, the sensor nodes are assumed to be stationary and densely deployed. Each sensor is assumed to be able to measure the range of the target. The range measurement noise of each sensor node is assumed to have Gaussian distribution.

The problem is divided into four sub-problems. The distributed implementation of Kalman filter is first proposed in conjunction with the least square trilateration algorithm: to reduce the tracking error and to save the power consumption of sensor nodes. Secondly, the uncertainty of trilateration algorithm is rigorously analyzed. Consequently, a set of minimum number of sensor nodes can be selected to track a target, still resulting in small tracking errors. Moreover, the use of a mobile robot can enhance the reliability of the tracking system because the mobile robot can be equipped with faster microcontrollers and longer battery life. The mobility of the mobile robot also eliminates the hand-over of the learned information between leader nodes, and the need to transmit data to the network sink. Finally, extending the life time of the network was studied by solving an optimization problem which maximized the network life time under the constraint of tracking performance.

1.4 Contributions

The contributions of the dissertation are as follows.

- A distributed tracking algorithm using Kalman filter was developed in a WSN to track a dynamic target. At any given instant, the Kalman filter is run on only one master node. The position and velocity of the target estimated by this filter are communicated to the nodes that are within the measurement range of the target. As the location of the target changes, a different node is selected to run the Kalman filter. The convergence of the proposed tracking algorithm is verified through mathematical proofs. Simulations examples are used to demonstrate the reduction in tracking error obtained by the proposed algorithm.
- The uncertainty in target position calculated using trilateration algorithm is formulated using a linearization based approach. The relationship between trilateration uncertainty and spatial distribution of the sensor nodes is exploited to design an algorithm to choose a minimum number of sensor nodes to track the target while still maintaining the required tracking quality.
- The hand-over of the Kalman filter from one master node to the next during the tracking of dynamic target is circumvented through the use of mobile robot. The estimated position and velocity of the target is used to determine the ground path for the robot. The robot carries the master node that executes the Kalman filter and the communication device for transmitting the estimated data to a network sink. Offloading power intensive aspect of target tracking is shown to reduce energy expenditure and prolong the useful life of a WSN.

- An optimization based approach to the maximization of the life time of the WSN while still maintaining a required tracking performance is also proposed. The algorithm selects the sensors with larger residual power and deactivates the sensors whose residual power is low. This approach is shown to reduce loss of coverage and increase the lifetime of the network.

1.5 Organization

In Chapter 2, the target tracking system using WSNs is studied. The application of WSNs in target tracking is first reviewed. Two classes of Kalman filter based approaches are then covered. Consequently, a new method for implementing distributed Kalman filter in tracking applications using WSNs is proposed. The stability and tracking error of the proposed technique are rigorously analyzed. Numerical simulations are used to demonstrate the reduction in power consumption.

The estimate of uncertainty in target position determined by trilateration algorithm will be studied in Chapter 3. If the range measurement of each sensor node is corrupted with white Gaussian noise, then the uncertainty in the position computed by the trilateration algorithm is compounded. Therefore, a formula is derived for calculating the uncertainty resulting from the trilateration approach when two or more sensors are used. A procedure to select a group of sensors that results in minimum trilateration uncertainty is then proposed.

In Chapter 4, the use of a mobile robot in conjunction with stationary sensor nodes is proposed. The current use of mobile robots in surveillance, perimeter patrol and target tracking is briefly surveyed. In the approach adopted in this chapter, the robot is assumed to carry the master node that executes the Kalman filter and the communication device for transmitting the estimated data to a network sink. A path planning strategy for the mobile robot is then developed to maintain the robot within one communication hop from the nodes sensing the target. Offloading power intensive aspect of target tracking is shown to reduce energy expenditure and prolong the useful life of a WSN.

In Chapter 5, the problem of enhancing the life time of a WSN in target tracking applications will be investigated. In this chapter, the problem is cast as an optimization problem where the life time of the sensor network is maximized under the constraints of tracking performance. The algorithm selects the sensors with larger residual power and deactivates the sensors whose residual power is low. To avoid the combinatorial problem associated with the selection of the nodes, the collinear elimination process is used to reduce the number of sensors, and a heuristic search algorithm is used to find the optimal solution. Numerical examples are used to demonstrate the effectiveness of the proposed algorithm.

Chapter 6 concludes the dissertation and discusses the future work.

Chapter 2

Stability and Performance of Wireless Sensor Networks during the Tracking of Dynamic Targets

The performance of Wireless Sensor Networks (WSNs) during the tracking of dynamic targets is addressed in this chapter. The problem of tracking targets using a WSN is first formulated. The minimum number of sensors required to track the target is selected and the location of the target is ascertained using the trilateration algorithm. A distributed implementation of a Kalman filter is then used to track the target. In contrast to the results reported in the literature, the approach in this chapter has the Kalman filter running on only one network node at any given time. The knowledge about the target acquired by this node, i.e., the system states and the covariance matrix, is passed on to the subsequent node running the filter. Since a finite subset of the sensor nodes is active at any given time, target tracking can be accomplished using lower power compared to centralized implementations of Kalman filter.

2.1 Introduction

Surveillance of remote inaccessible areas and the detection and tracking of intruders are some of the important applications of Wireless Sensor Networks (WSNs). Research in WSNs has addressed several important issues in optimal deployment, coverage, routing, and energy efficiency of the WSNs [1, 7, 10, 11, 19, 89]. Diffusion and directed diffusion approaches have been proposed to address coverage, route discovery, routing, and sensing fusion issues in WSNs [31]. The applications of WSNs in surveillance and monitoring of target areas have also been widely researched [47]. While the results presented in these papers are encouraging, their applicability in low cost WSNs with large measurement noise and faulty measurements is fraught with problems. In recent years, Kalman filters have been used to address the uncertainty and the measurement in WSNs [66-72]. The convergence analysis of extended Kalman filters was also studied by several researchers [62, 90]. Both centralized and distributed implementation of the Kalman filter was proposed to make their use suitable to WSN applications. However, these techniques are still power intensive and require significant amounts of onboard power for computing the location of the target and communicating the information among sensor nodes and to the network sink.

Two classes of Kalman filters have been implemented in WSNs to address the problem of tracking targets. In the first approach, centralized implementation of Kalman Filter was pursued [72]. In this approach, every sensor node is active and communicates its measurements to a central node in the network. The Kalman filter is implemented on the central node and computes the estimated location of the target using the measurements from all the active nodes. In this approach, the residual power of the nodes will be depleted quickly due to unnecessary measurements and inter-node communication. Moreover, it is sometimes impractical for a sensor node to communicate with all other nodes due to limitation of communication ranges. Addressing redundancies and latencies in reported measurements arising out of multi-hop communication is also problematic.

The use of distributed Kalman filters was the second approach proposed in literature to address target tracking using WSNs [66, 70, 71]. In this approach, every neighbor node runs its own version of Kalman filter and shares the information with its neighbors. The estimates from all the filters are used to reach the consensus location of the target. The approaches are more efficient compared to the centralized implementation of the Kaman Filter. However, the efficiency obtained depends on the number of neighbor nodes that are active at any given instant and the complexity of the consensus algorithm. Consequently, these approaches have not been widely used for tracking targets using WSNs.

In this chapter, the distributed Kalman filter is implemented to estimate the position of the target. The approach is different from the above two techniques in the sense that the Kalman filter is implemented in a distributed fashion across the WSNs. At a given instant, only one master node runs the Kalman filter using the measurements from its neighbors and shares the estimated knowledge with the subsequent master node. The neighbors within a certain distance from the target measure the distance to the target, and transmit measurements to the master node. On one hand, the procedure significantly reduces the communication costs among the neighbor nodes in comparison to the algorithms reported elsewhere in the literature. On the other hand, since the master node alone executes the Kalman filter and the neighbor nodes only perform measurement functions, the complexity of the WSN is greatly reduced. This results in lower communication costs in the entire network and reduced complexity of the tracking algorithm.

The approach proposed in this chapter was validated through mathematical analysis and simulation examples. The algorithm was also able to track the target with random directions with acceptable estimated results. The numerical examples showed that this method is robust to measurement noise and changes in velocity. The estimated knowledge of the Kalman filter including system states and covariance matrix are passed directly to the subsequent master node where the execution of the Kalman filter is transitioned to. Another aspect of the proposed algorithm is that the master node determines the direction and velocity of the intruder and wakes up appropriate sensor nodes in the direction of the target travel. Thus, nodes further away from the target are inactive and only a small subset of the nodes participates in sensing. Prior to the start of the tracking, the knowledge of the maximum target velocity can be used to activate the nodes along the boundary in a round-robin fashion in order to save energy [1].

2.2 Problem Formulation

A closed and bounded sensor field in three-dimensional (3D) Cartesian coordinate system is densely deployed with stationary sensor nodes. Each node is equipped with a computational platform, and a wireless transceiver with a predetermined communication range. Nodes within a known sensing range can detect the presence of a target, measuring the distance between the target and itself, and determining their source of power. The sensing capability of each sensor is assumed to be omnidirectional. The tracking problem can then be stated as (1) the detection of the entry of an intruder into the surveillance region; and (2) tracking the possibly nonlinear trajectory of motion of the intruder within this region.

At time instant k, the dynamics of the target is assumed to satisfy the following equations:

$$x_{k+1} = f(x_k, w_k) \tag{2.1}$$

$$y_{k+1} = h(x_k, \mu_k). \tag{2.2}$$

Where $x_k = [x_k^1; x_k^2] \in \mathbb{R}^6$ is the state of the target; $x_k^1 \in \mathbb{R}^3$ and $x_k^2 \in \mathbb{R}^3$ represent the velocity and position, respectively in a 3D coordinate system. $w_k \sim \mathcal{N}(0, Q_k)$ is zero mean state noise with covariance matrix Q_k, which is assumed to be positive semidefinite. μ_k is the measurement noise, which will be discussed in detail in the next subsection. The state equation f and the measurement equation h are assumed to be continuous with respect to time and at least twice differentiable with respect to x_k. If the maximum velocity of a target is known, the domain $\mathcal{D} \subseteq \mathbb{R}^6$ of $f(x_k, w_k)$ in (1.1) is a compact and connected set.

2.2.1 Measurement Model and Trilateration Algorithm

Suppose that at time k, the position of i^{th} sensor is $c_i \in \mathbb{R}^3$, and its range measurement to the target $d_i \in \mathbb{R}$ is corrupted by white Gaussian noise $\mu_i \sim \mathcal{N}(0, \sigma_V^2)$. The position of the target is $T_k \in \mathbb{R}^3$, and the measurement model is given by the following equation

$$d_i = \|c_i - T_k\|_2 + \mu_i, \tag{2.3}$$

where $\|.\|_2$ is the standard Euclidean norm. Assuming that there are n_k sensors that can sense the target, there are n_k nonlinear measurement equations in the form of (2.3). For each pair of integers (i, j), $1 \leq i \neq j \leq n_k$, the i^{th} and j^{th} equations in (2.3) are squared and subtracted to represent the measurements in the following form

$$A_k T_k = r_k \tag{2.4}$$

where A_k is $M \times 3$ matrix, $M = \frac{n_k(n_k-1)}{2}$, while r_k is $M \times 1$ column matrix. In (2.4), t^{th} row of A_k and r_k in equation (2.4) are given by

$$A_{k_t} = 2(c_i - c_j)$$
$$r_{k_t} = (d_i - \mu_i)^2 - (\|c_i\|_2 - (d_j - \mu_j)^2 + \|c_j\|_2).$$

where $t = \varphi(i,j)$. The map $\varphi: [1 \div n_k] \times [1 \div n_k] \mapsto [1 \div M]$ is any one-to-one. Consequently, $A_k = [A_{k_1} A_{k_2} \dots A_{k_M}]^T$ and $r_k = [r_{k_1} r_{k_2} \dots r_{k_M}]^T$

The least square solution of the trilateration algorithm (2.4) is given by

$$y_k = T_k = (A_k^T A_k)^{-1} A_k^T r_k. \tag{2.5}$$

The measurement equation (5) can be linearized as

$$y_k = H_k x_k + \theta_k \tag{2.6}$$

where $y_k \in \mathbb{R}^3$ is the measured position of the target, and $\theta_k \in \mathbb{R}^3$ is jointly uncertainty with covariance matrix $\Theta_k \in \mathbb{R}^{3\times3}$, and the relationship between θ_k and μ_k is described by (2.3), (2.5) and (2.6). The measurement matrix H_k is given by

$$H_k = \begin{bmatrix} 0 & 0 & 0 & 1 & 0 & 0 \\ 0 & 0 & 0 & 0 & 1 & 0 \\ 0 & 0 & 0 & 0 & 0 & 1 \end{bmatrix}.$$

Since H_k is a constant matrix, from now on the subscript k is dropped to simplify the notation, i.e., $H = H_k$.

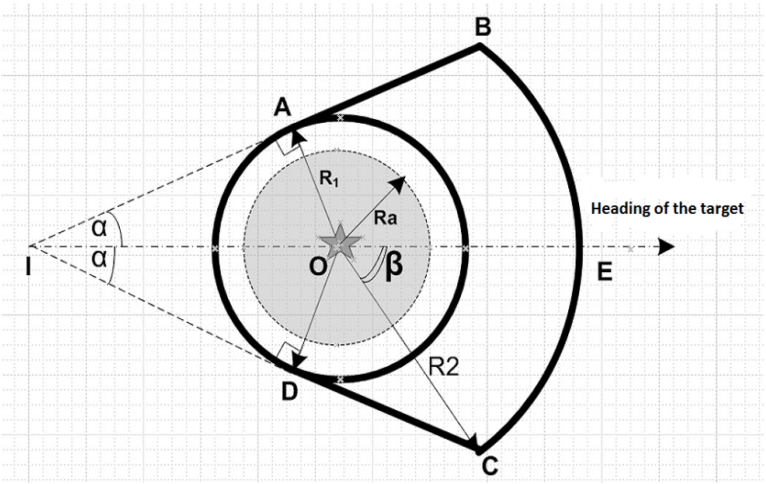

Figure 2.1: Region of Activation $\boldsymbol{\mathcal{R}}$

2.2.2 Distributed Implementation of Kalman Filters

Suppose that the target, represented by ⋆ symbol in Figure 2.1, is moving in the direction of vector $\overrightarrow{OE}$. The region $\boldsymbol{\mathcal{R}}$ is defined by the sphere of radius R_1, the radius of R_2 and angle 2α – the region limited by the bold lines. R_2, R_1, and R_a $(R_2 > R_1 > R_a)$ are activation radius, sensing radius, and measurement radius of sensor nodes respectively. Figure 2.1 shows the projection of the region $\boldsymbol{\mathcal{R}}$ onto a horizontal plane (on which the heading of the target lies). All the sensor nodes inside the region of activation $\boldsymbol{\mathcal{R}}$ are activated, while the nodes outside the region are in sleep mode in order to conserve power. All the nodes inside the sphere (O, R_1) can sense the target while no node outside this sphere can detect the target. However, only nodes inside the sphere $(O,\ R_a)$ are actively taking measurements and reporting the data to the master node.

A master node is selected depending on two criteria: its distance to the target and its residual power. The sensors, inside the sphere with radius R_a, measure the distance to the target and transfer the range measurements to the master node. The master node runs the extended Kalman filter for the system (2.1) and (2.2) in a distributed sense, obtaining the estimated position and direction of the target, broadcasting the learned information to its neighbors. After receiving the information, a neighbor node will turn on or off depending on whether it is inside or outside region $\mathcal{R}$.

$$\hat{x}_{k+1} = \hat{x}_{k+1|k} + K_{k+1}(y_{k+1} - H\hat{x}_{k+1|k}) \tag{2.7}$$

$$K_{k+1} = P_{k+1|k}H^T(HP_{k+1|k}H^T + \Theta_k)^{-1} \tag{2.8}$$

$$P_{k+1} = (I - K_{k+1}H)P_{k+1|k} \tag{2.9}$$

$$\hat{x}_{k+1|k} = f(\hat{x}_k, 0) \tag{2.10}$$

$$P_{k+1|k} = FP_kF^T + W_kQ_kW_k^T \tag{2.11}$$

$$F_k = \frac{\partial f(x_k)}{\partial x_k}|_{x_k=\widehat{x_k}} \tag{2.12}$$

$$W_k = \frac{\partial f(x_k)}{\partial w_k}|_{x_k=\widehat{x_k}} \tag{2.13}$$

The target is represented by ⋆ at point O. The boundary of the region of activation $\mathcal{R}$ is limited by line AB, curve BEC, line CD and curve DA. The curve BEC is formed by part of the sphere (O, R_2). The extended Kalman filter is run on a master node according to the system equations (2.1) and (2.6).

While the equations (2.7)-(2.9) reflect measurement updates, the equations (2.10)-(2.13) reflect time updates for the Kalman filter. F_k is the Jacobian matrix of function f

in (2.1) at time k. P_0, the initial value of P_k in (2.11), is a symmetric positive semidefinite matrix. If the sampling time Δt is fixed, F_k in (2.12) is a time invariant matrix. For simplicity in notation, the subscript k is dropped and the matrix F is represented as

$$F = F_k = \begin{bmatrix} 1 & 0 & 0 & 0 & 0 & 0 \\ 0 & 1 & 0 & 0 & 0 & 0 \\ 0 & 0 & 1 & 0 & 0 & 0 \\ \Delta t & 0 & 0 & 1 & 0 & 0 \\ 0 & \Delta t & 0 & 0 & 1 & 0 \\ 0 & 0 & \Delta t & 0 & 0 & 1 \end{bmatrix}.$$

By adopting a constant velocity model [91], the Jacobian matrix, W_k , of derivative of f with respected to w_k in (2.13) is given by

$$W_k = \begin{bmatrix} \Delta t & 0 & 0 \\ 0 & \Delta t & 0 \\ 0 & 0 & \Delta t \\ \frac{\Delta t^2}{2} & 0 & 0 \\ 0 & \frac{\Delta t^2}{2} & 0 \\ 0 & 0 & \frac{\Delta t^2}{2} \end{bmatrix}.$$

2.3 Performance Analysis

2.3.1 Assumptions

The following assumptions are made to facilitate the stability analysis of the tracking system

(i) Function $f(x_k, w_k)$ in (2.1) is twice differentiable with respect to x_k.

(ii) The state error in (2.1) has a Gaussian distribution with a covariance matrix Q_k that is uniformly bounded.

(iii) The range measurement error μ_i in (2.3) has a Gaussian distribution.

(iv) The sensor nodes are densely deployed so that the joint measurement error θ_k in (2.6) can be represented by a Gaussian distribution with zero mean and joint measurement covariance matrix Θ_k that is uniformly bounded.

(v) The transition of the Kalman filter from one Master Node to the next can be achieved within one sample instant.

(vi) The clocks of all sensing nodes are synchronized.

(vii) Every node active during the sensing cycle is within one hop to the master node.

2.3.2 Stability Analysis

In this section, we analyze the convergence of the Kalman filter. A Lyapunov candidate function is chosen, which is positive semidefinite. The tracking errors converge when observability of the system (F_k, H_k) and the bounded conditions on the trilateration uncertainty are met.

Equation (2.1) can be linearized as follows.

$$x_{k+1} = Fx_k + \Delta F_k x_k + w_k = a_k F x_k + w_k, \tag{2.14}$$

where ΔF_k and a_k are the diagonal matrices representing the nonlinear terms. If the system (2.1) is linear, $\Delta F_k = 0$ and a_k is an identity matrix.

The Lyapunov function candidate is chosen as

$$V_{k+1} = \tilde{x}_{k+1}^T P_{k+1}^{-1} \tilde{x}_{k+1} \tag{2.15}$$

where $\tilde{x}_{k+1} = x_{k+1} - \hat{x}_{k+1}$.

Let $\tilde{x}_{k+1|k} = \hat{x}_{k+1|k} - x_{k+1}$, and from (2.14) we have

$$\tilde{x}_{k+1|k} = [a_k F \hat{x}_k + w_k] - [a_k F x_k + w_k] = a_k F \tilde{x}_k. \tag{2.16}$$

Let

$$e_{k+1} = y_{k+1} - Fx_{k+1|k} = H\tilde{x}_{k+1|k}. \tag{2.17}$$

Then, from (2.7)-(2.13) and assumption (i) we have

$$\begin{aligned} V_{k+1} &= \left(\tilde{x}_{k+1|k} - P_{k+1}H\Theta_k^{-1}e_{k+1}\right)^T P_{k+_1}^{-1}\left(\tilde{x}_{k+1|k} - P_{k+1}H\Theta_k^{-1}e_{k+1}\right) \\ &= \tilde{x}_{k+1|k}^T P_{k+1}^{-1}\tilde{x}_{k+1|k} - e_{k+1}^T[\Theta_k^{-1}H^T P_{k+1}H\Theta_k^{-1} - 2\Theta_k^{-1}]e_{k+1} \end{aligned} \tag{2.18}$$

From (2.8), (2.9) and (2.11) we have $P_{k+1}^{-1} = P_{k+1|k}^{-1} + H\Theta_k^{-1}H^T$

$$\begin{aligned} &\Delta V_k = V_{k+1} - V_k \\ &= \tilde{x}_k^T[F^T a_k^T(FP_kF^T + \mathrm{W}_kQ_k\mathrm{W}_k^T)^{-1}a_kF - P_k^{-1}]\tilde{x}_k e_{k+1}^T\Theta_k^{-1}(HP_{k+1}H^T\Theta_k)\Theta_k^{-1}e_{k+1} \\ &= (F\tilde{x}_k)^T[a_k^T(FP_kF^T + \mathrm{W}_kQ_k\mathrm{W}_k^T)^{-1}a_k - (FP_kF^T)^{-1}]F\tilde{x}_k \\ &\qquad\qquad + e_{k+1}^T\Theta_k^{-1}(HP_{k+1}H^T - \Theta_k)\Theta_k^{-1}e_{k+1} \end{aligned} \tag{2.19}$$

For any vector m we have

$$\begin{aligned} &m^T[a_k^T(FP_kF^T + \mathrm{W}_kQ_k\mathrm{W}_k^T)^{-1}a_k - (FP_kF^T)^{-1}]m \leq \\ &\leq \lambda_{max}((FP_kF^T + \mathrm{W}_kQ_k\mathrm{W}_k^T)^{-1})\|a_k\|^2\|m\|^2 - \lambda_{min}((FP_kF^T)^{-1})\|m\|^2 \end{aligned} \tag{2.20}$$

Thus, if

$$HP_{k+1}H^T - \Theta_k \leq 0 \quad \text{and} \tag{2.21}$$

$$\lambda_{max}(a_k) \leq \frac{\lambda_{min}((FP_kF^T)^{-1})}{\lambda_{max}((FP_kF^T + \mathrm{W}_kQ_k\mathrm{W}_k^T)^{-1}} \tag{2.22}$$

Then $\Delta V_k \leq 0$. On the other hand, the matrix

$$O_k = \begin{bmatrix} H \\ HF \\ \vdots \\ HF^{n-1} \end{bmatrix} \text{ where } \begin{bmatrix} H \\ HF \end{bmatrix} = \begin{bmatrix} 0 & 0 & 0 & 1 & 0 & 0 \\ 0 & 0 & 0 & 0 & 1 & 0 \\ 0 & 0 & 0 & 0 & 0 & 1 \\ \Delta t & 0 & 0 & 1 & 0 & 0 \\ 0 & \Delta t & 0 & 0 & 1 & 0 \\ 0 & 0 & \Delta t & 0 & 0 & 1 \end{bmatrix}$$

Since O_k is full rank, and F_k and H_k are observable. Hence, by LaSalle's invariance principle [92], we conclude that

$$\lim_{k\to\infty} \tilde{x}_{k+1} = 0. \qquad (2.23)$$

The equation (2.23) means that the expectation of the estimated error goes to zero as k goes to infinity. However, the variance of the estimated error depends on the variance of the tracking system, i.e., the uncertainty of trilateration algorithm Θ_k and the nonlinearity of the target trajectory a_k.

2.4 Discussion

The statistics of the range measurements noise in (2.3) is assumed to be Gaussian. However, this does not necessarily mean that the joint distribution in (2.6) is either Gaussian or zero mean. In this subsection, it is shown that if the sensors are deployed dense enough, then the joint measurement error θ_k (2.6) is bounded and can be approximated as a Gaussian distribution. The joint distribution depends not only on the range measurement noise but also on the spatial distribution of the sensor nodes and the target.

Suppose that the maximum sensing radius and range measurement error of each node is represented by R_S and u respectively. Further, if the probability that measurement error is smaller than u is p, then the target is in the shaded region in Figure 2.1a with the probability of p. When the target is covered by one sensor, its maximum uncertainty is $R_S + u$. When the target is covered by two sensors, its maximum uncertainty is

$$l = \sqrt[2]{\left(\frac{d}{2}\right)^2 - R_s^2} \tag{2.24}$$

where $d = S_1S_2 \leq 2R_S$ is the distance between two sensor nodes. The probability that the target lies in either one of the two shading regions in Figure 2.2b is p^2. The following theorem then yields a bound on the area of each shaded regions.

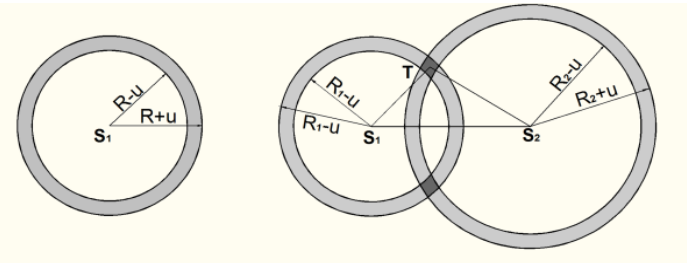

Figure 2.2: The uncertainty in measurement when the target is covered by one sensor (a) and two sensors (b)

Theorem 1.1: Suppose that the target T is covered by two sensor nodes S_1 and S_2, and the angle at T formed by two vertices S_1, and S_2 is $\widehat{S_1TS_2} = \alpha.$ The maximum uncertainty of the target in one region is (one shaded region 2.2Error! Not a valid bookmark self-reference.b):

$$l \leq min\left\{\frac{2\sqrt{2}u}{sin\frac{\propto}{2}}; R + u\right\}, \tag{2.25}$$

The first term in (2.25) can be easily verified through geometric calculations. The second term is the maximum uncertainty of a target represented in Error! Not a valid bookmark self-reference.a.

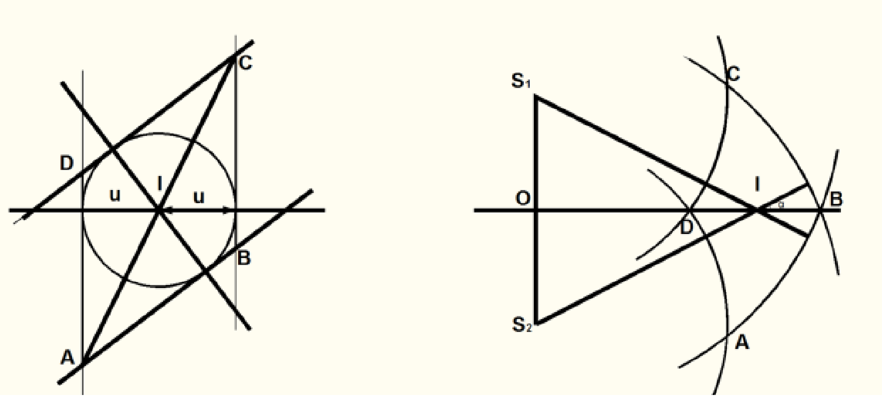

Figure 2.3: Measurement uncertainty when distances to the target are (a) large (b) small.

In Figure 2.2a, as R goes to ∞, the upper bound on uncertainty is reached:

$$l = \frac{2u}{sin\frac{\alpha}{2}} \tag{2.26}$$

In short, the joint measurement uncertainty depends on both sensor measured uncertainty u and the angle α. Thus, if u is given, sensor nodes can be deployed densely enough so that $sin\frac{\alpha}{2}$ is within a certain bound. By Theorem 1.1, the measurement noise covariance matrix Θ_k is uniformly bounded.

The choice of the master node is determined by both the normalized residual power ($P_{residual}$) of each node and its distance to the target. At each instant, every active node, within the proximity of the target, computes the weighted sum of its residual power ($P_{residual}$) and its normalized distance to the target (*D*) as follows: $W = \alpha D + \beta(1 - P_{residual})$ with $\alpha, \beta \in [0,1]$, and $\alpha + \beta = 1$. As $\alpha \rightarrow 1$, the weighted sum depends greatly on the distance to target. Meanwhile, as $\beta \rightarrow 1$, the weighted sum is affected mainly by the residual power. A node will become the new master node if its weighted sum is smaller than that of the current master node. Consequently, the current master node transfers knowledge of the Kalman filter (i.e., measurement covariance matrix and state of the target) to the new one.

2.5 Numerical Examples

In this section, several numerical examples are presented to demonstrate the effectiveness of WSN in tracking dynamic targets. First, a power consumption model similar to the one proposed in [1] is assumed for the radio communications between individual sensor nodes. Several scenarios are considered to study the performance improvement obtained and the tracking error.

2.5.1 Power Consumption Model

To demonstrate the effectiveness of our approach, the power analysis in [1] was used without assuming any specific hardware platform for the numerical examples. The transmitted power P_{Tx}, received power P_{Rx}, idle power P_i and sleeping power P_s are *1400 mW, 1000 mW, 830 mW*, and *130 mW* respectively. Let n_a be the number of sensor nodes inside sphere radius R_a; n_i be outside the sphere R_a but inside the region $\boldsymbol{\mathcal{R}}$. Let n be total number of sensor nodes; n_b be number of active ones. The total power consumption of the sensor field in one sampling cycle is calculated as following.

The n_a neighbors make n_a transmissions and the master node receives n_a times.

$$P_{meas} = n_a(P_{Tx} + P_{Rx}) \tag{2.27}$$

The master node broadcasts the target position and its directions, and it makes one transmission. Each of $(n_a + n_i)$ neighbors in the cone area receives the information of the target once.

$$P_{broadcast} = (n_a + n_i)P_{Rx} + P_{Tx} \tag{2.28}$$

Each active node, except measurement nodes, consumes an amount of the idle energy

$$P_{idle} = (n_b + n_i)P_i \tag{2.29}$$

The other nodes are sleeping, and the total power consumed by these nodes is

$$P_{sleep} = (n - n_a - n_i - n_b)P_s \tag{2.30}$$

Then total consumed power is

$$P_w = P_{meas} + P_{broadcast} + P_{idle} + P_{sleep} \tag{2.31}$$

2.5.2 Simulation

We considered two scenarios to demonstrate the distributed Kalman filter for target tracking using a WSN. In the first scenario, sensor nodes were assumed to be uniformly distributed. This requirement was relaxed in the second scenario where the nodes were randomly deployed. It was further assumed that no hole in coverage existed within the regions to be monitored, and every point was covered by at least three sensors. The sensor field was a square of 10×10 units as seen in Figure 2.. By choosing the distance of any two closest nodes to be 0.5 units, the total number of uniformly distributed sensor nodes was 441. The target was assumed to move along the horizontal trajectory with the sinusoid velocity profile while the vertical coordinate remains at $y = 5$. In 10 seconds, the target traveled between the coordinates $(0, 5)$ and $(10, 5)$, and the sampling frequency was $200\ Hz$. The following difference equations were used to model the dynamic behaviors of the moving target.

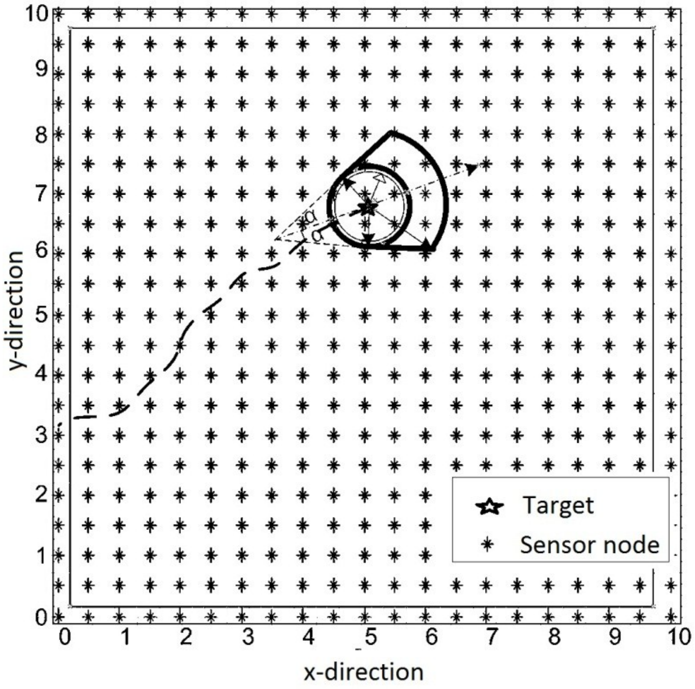

Figure 2.4: Example of sensor field and the trajectory of the target

$$\begin{aligned} x_{k+1} &= Fx_k + w_k \\ y_k &= Hx_k + \theta_k \end{aligned} \qquad (2.32)$$

Where $F = \begin{bmatrix} 1 & 0 \\ \Delta t & 1 \end{bmatrix}$, $x_k = \begin{bmatrix} x_k^1 \\ x_k^2 \end{bmatrix}$, $H = [0 \;\; 1]$

x_k^1 is the target velocity and; x_k^2 is target position in x-direction at time k. Δt is the sampling time. Moreover, w_k and θ_k were state noise and measurement noise. From scenario 1 to scenario 4, the initial condition for the Kalman filter was the same as the true value while it was nonzero in scenario 5. The sensor nodes were uniformly deployed in scenario 1 to scenario 5 while randomly deployed in scenario 6.

Scenario 1: Without using the Kalman filter, more sensors used in measurement results in better estimated tracking. As seen in Table 2.1, when the average measured sensor nodes increased from 4.5 to 17.5, the noise variance decreased from 21.71×10^{-3} to 13.49×10^{-3}. However, the trade off was the total power consumption of the network increased from 1.38×105 to 2.09×105 (mW). The power consumption analysis is shown in Figure 2.5.

Table 2.1: Performance analysis

Average measured sensors	Average active sensors	Error variance without Kalman filter ($\times 10^{-3}$)	Error variance with Kalman filter ($\times 10^{-3}$)	Average total power consumption (mW × 10^{5})
4.5	9.3	24.71	3.63	1.38
17.5	39.2	13.49	1.57	2.09
60.4	139.9	7.03	0.98	4.48
130.8	275.5	4.62	0.31	7.88
279.1	416.2	5.43	0.10	12.60

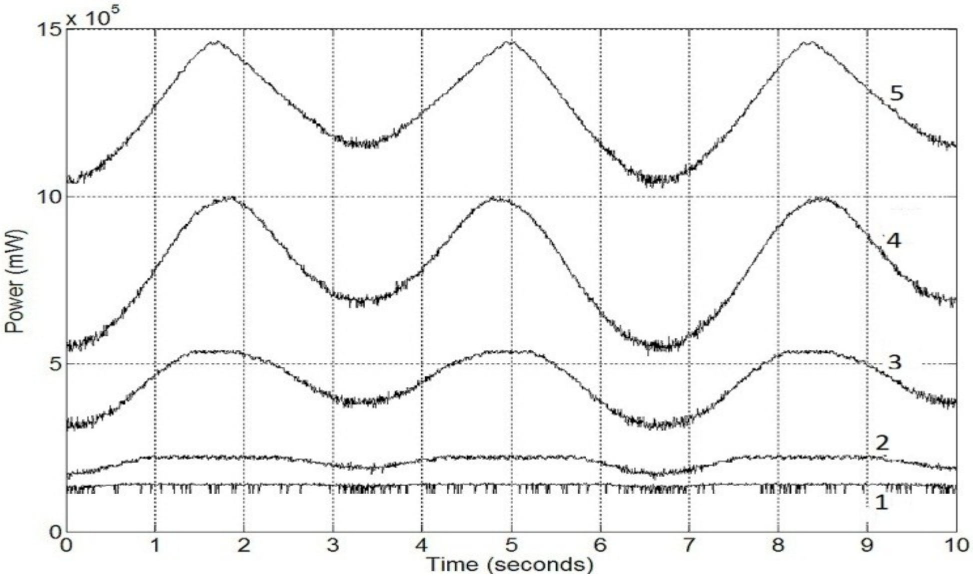

Figure 2.5: Power consumption during (uniform distribution of sensor nodes)

In Figure 2.5, without the Kalman filter, the lines numbered 1, 2, 3, 4, and 5 have average measured sensor nodes of 4.5, 17.5, 60.4, 130.8, and 279 respectively. For the lines numbered from 3 to 5, the total power consumption fluctuated because when the target moved close to the boundary, the decrease in the number of active sensors results in smaller total power consumption. Line #1 and #2 were reasonably flat because in these cases, the relatively small regions of activation $\boldsymbol{\mathcal{R}}$ result in fewer active sensors irrespective of location of the target in the sensor field.

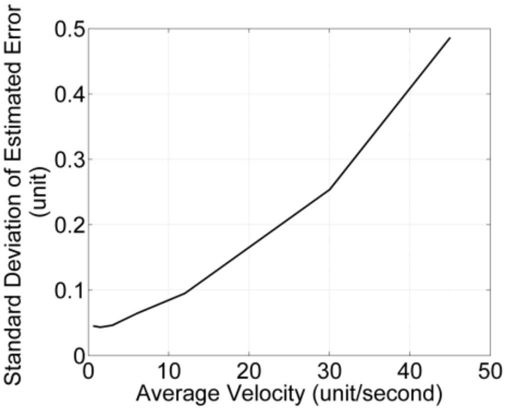

Figure 2.6: Average velocity and standard deviation of estimated error.

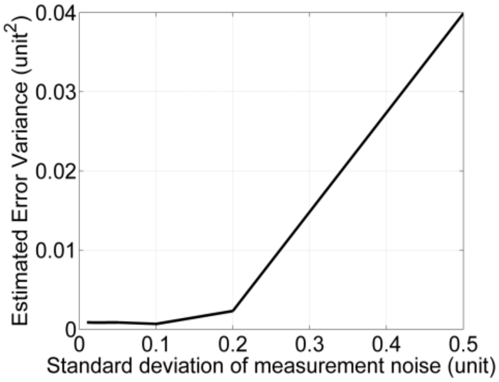

Figure 2.7: Standard deviation of measurement noise and estimated error variance

As the average velocity increased in Figure 2.6, the estimated error had larger standard deviation. In Figure 2.7, when the measurement was subjected to a larger noise, the variance of the estimated tracking error increased.

Scenario 2: When the Kalman filter was used, the variance of the estimated error was smaller and Figure 4 shows the smoother tracking performance compared to scenario 1. As shown in Table 2.1, by using the Kalman filter, only an average of 4.5 measured sensors was sufficient to achieve the error variance of 3.63×10^{-3} which was smaller than 5.43×10^{-3} resulted by an average of 279.1 measured sensors without using Kalman filtering.

Scenario 3: When the number of average measured sensors and the sampling frequency were fixed, slower average velocity resulted in smaller estimated tracking error as shown in Figure 2.6. In this scenario, the sampling frequency is 200Hz, the standard deviation of state noise and measurement noise were 0.01 and 0.2 respectively, and the average number of measured sensors was 6.3.

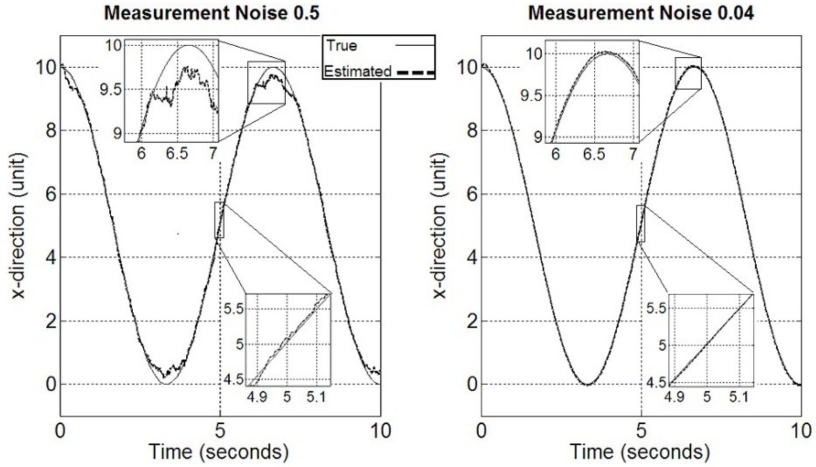

Figure 2.8: The true and the estimated trajectory with different measurement noise levels. The standard deviation of measurement noise is 0.5 on the left side while it is 0.04 on the right side.

Scenario 4: In this scenario, the sampling frequency was kept at $200\ Hz$, average target velocity was three units per second, and the average number of measured sensors was 6.5. In Figure 2.7, the standard deviation of state noise is fixed at 0.01 while the measurement noise has a standard deviation varying from 0.01 to 0.5. The variance of estimated error increased with the increase in measurement noise. In addition, with the same number of average measured sensors of 6.5, the smaller measurement noise leaded to the better tracking performance. The tracking performance, shown in Figure 7, was better when the measurement noise is smaller.

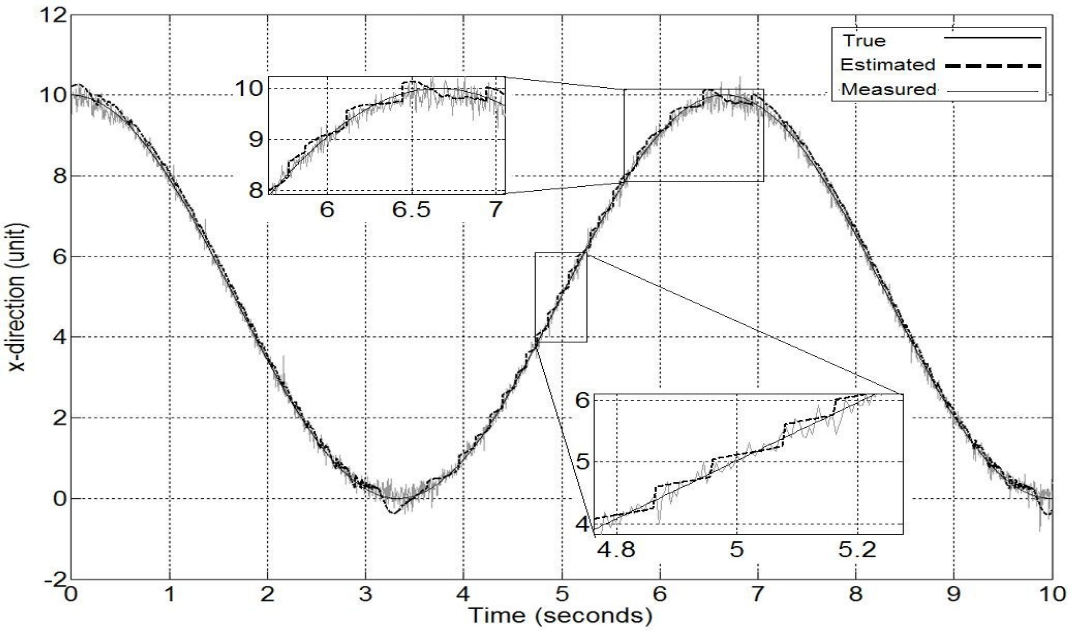

Figure 2.9: True, estimated, and measured trajectory of the target without sharing covariance matrix and state vector to the subsequent master node vs. time**.**

Scenario 5: When the master node did not share the knowledge of the target (i.e., the target state and the covariance matrix) with the subsequent one, which has to run the Kalman filter from the default initial conditions. The change in master nodes was indicated by the abrupt jumps in estimated error as shown in Figure 2.9, and the Kalman filter required some extra time steps to converge. The measurement noise standard deviation was 0.2, while the number of average measured sensor nodes was 7.6.

In Figure 2.10, the target's true trajectory was the solid black line, and its estimations using trilateration with the Kalman filter and without the Kalman filter were the solid gray line and the dashed black line respectively. The average number of measured sensors was 4.5, and the standard deviation of state noise and measurement noise were

0.01 and 0.2 respectively. The Kalman filter yielded both a smaller error variance and smoother estimated trajectory. As we zoomed in two small sub figures, the estimated position was close to the true position when the target moves in a linear part of the sinusoid trajectory. Without using the Kalman filter, the estimated trajectory was noisy.

Scenario 6: As shown in Figure 2.11, when the sensor nodes were randomly distributed, similar results in comparison to the uniform scenario shown were observed in Figure 2.5. However, the power consumption line was not as smooth as it was in the uniform scenario. Due to the random nature, more sensor nodes covered a specific point while fewer sensor nodes covered other points. In order for our algorithm to work effectively, at least three sensor nodes had to cover each point in the sensor field.

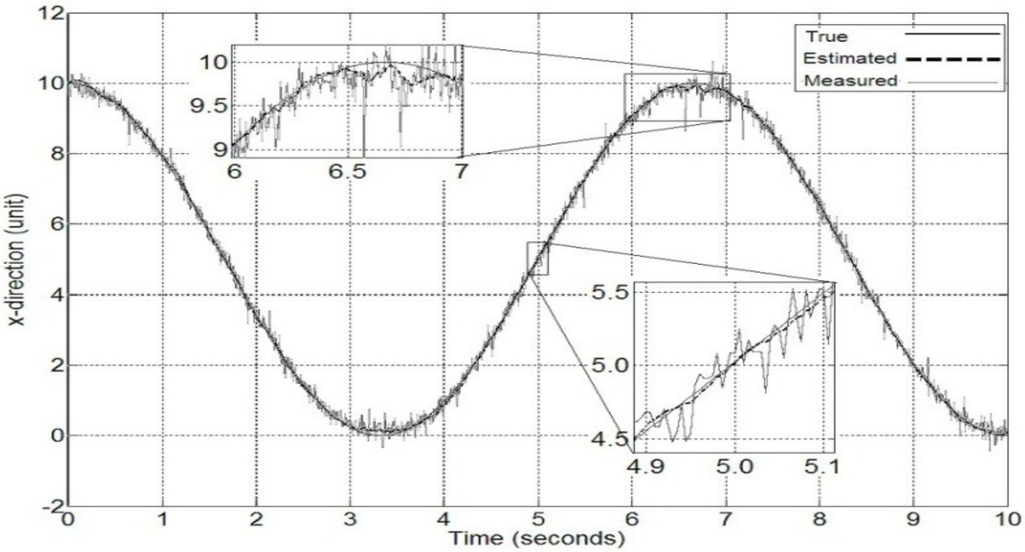

Figure 2.10: Tracking performance with and without the Kalman filter

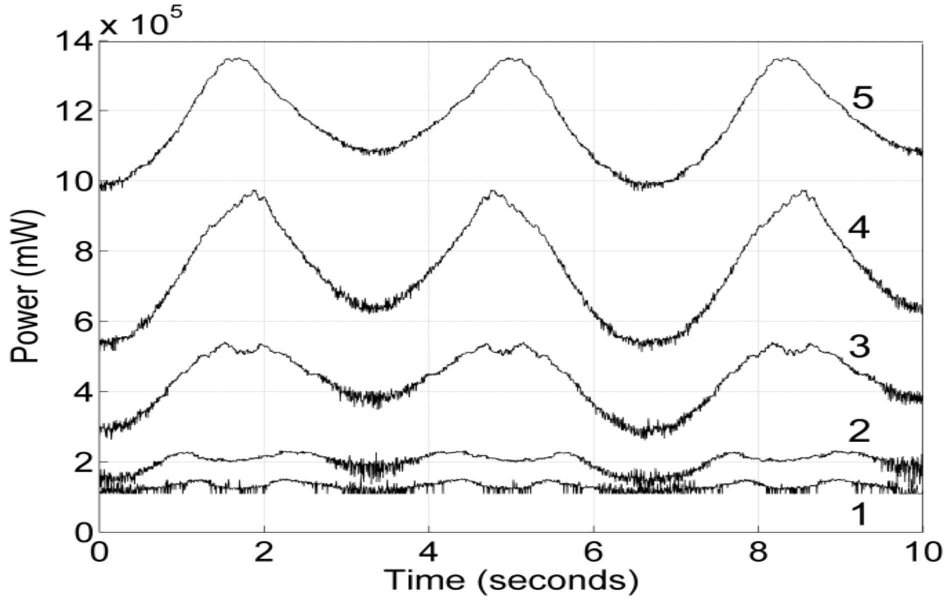

Figure 2.11: Power consumption of one sampling cycle in random deployment

In Figure 2.11, the lines labeled 1, 2, 3, 4 and 5 have average measured sensors of 3.4, 15.7 59.5, 127.2, and 259.7 respectively. Similar to the uniform deployment case, the more number of nodes were used for tracking, the higher power is consumed.

The above results show that a distributed implementation of Kalman filter in a WSN was successful in tracking moving targets. The tracking error was small when the target follows a linear trajectory while nonlinear trajectories with high target velocities resulted in higher tracking errors. However, in all these scenarios, the tracking error was 12.5% smaller than that obtained in the absence of the Kalman filter. In addition to the improved tracking performance, the distributed filter required fewer nodes to be active at any given instant, thereby reducing the overall power consumption of the WSN. This is significant because the lower power consumption increases the useful life of the WSN.

2.6 Conclusion

In this chapter, a distributed computation approach was proposed for tracking dynamic targets using a Wireless Sensor Network (WSN). The tracking problem was mathematically formulated and the tracking error of the distributed Kalman filter was rigorously analyzed. It is shown that the proposed algorithm is stable and can track the target with predetermined error bounds on the performance. The algorithm is also robust to changes in the velocity of the target and measurement noises. It was shown that the algorithm reduces the total power consumption in the network compared to similar algorithms reported in literature. The theoretical proofs and numerical simulations demonstrated the flexibility and power of the proposed tracking algorithm.

Chapter 3

Uncertainty of Trilateration Algorithm

In the previous chapter, the sensor nodes are assumed to be deployed densely so that each point in the sensor field is covered by a large number of sensor nodes. Consequently, the uncertainty of the trilateration algorithm is close to Gaussian distribution. In this chapter, we relax the assumption of closeness to Gaussian distribution, and choose a smaller number of sensor nodes for tracking while still maintaining the desired tracking performance. The trilateration uncertainty and its relationship to spatial distribution of sensor nodes are addressed and a sensor selection algorithm is proposed. Finally, Kalman filter is implemented to further improve tracking quality. The approach will be verified by mathematical analyses and numerical examples.

3.1 Introduction

Surveillance and monitoring have become important applications using Wireless Sensor Networks (WSNs). Tracking of a target using range-only sensors poses several challenges. The first challenge is to determine the trilateration uncertainty [84, 85] associated with the measurements from a set of sensor nodes. The second challenge is the selection algorithm [82, 83, 93] that activates a minimum number of sensors within the measurement range of the target that result in smallest localizing error. Therefore, both total power consumption and communication bandwidth can be reduced greatly. The third challenge is to implement the estimation techniques to further improve tracking quality in a distributed manner. Extending the useful life of WSNs by reducing the overall power consumption is another challenge that has to be addressed [31, 88].

Trilateration is an algorithm for estimating the coordinates of an object given the distances from it to known locations. The uncertainty in range measurements and the spatial locations of reference objects affect the accuracy of the algorithm. A number of methods have been proposed to improve the performance of trilateration algorithm: recursive formula [56], closed-form approach [50], joint covariance variance matrix [94], Clay-Menger determinant [53], among others. While these works analyzed the trilateration uncertainty comprehensively, the computation is complicated except in a few trivial cases. Additionally, most of the works used GPS data where the target, on the earth surface, lies in the center of a triangle formed by three satellites – resulting in smallest trilateration uncertainty. These analyses usually used only three reference objects to estimate position of a target while in a WSN four or more may be needed.

Several approaches for selecting sensor nodes to track the target in systems using bearing-only measurements have been proposed in [85, 88]. Selection of sensor nodes to balance between the tracking performance and constraints such as communication cost, energy consumption, and bandwidth has been proposed in [31, 84]. After the target is localized by techniques such as trilateration or triangulation, Kalman filters [66, 95] and particle filters [96] have been used for further reducing the tracking errors.

In this chapter, the trilateration uncertainty is analyzed using the linearization based method and the relationship between trilateration uncertainty and spatial distribution of sensor nodes is determined. This relationship is used in the selection of sensor nodes for tracking the target. The search algorithm uses the heuristic ranking and greedy technique which significantly reduce the computation required. The total power consumption and the communication bandwidth are also reduced thereby extending the useful life of the WSN. The approach is not computationally intensive and is suitable for low cost WSNs. More importantly, trilateration uncertainty can be taken into account during the selection of the sensors and improves the performance of estimation techniques [70, 72, 97].

While trilateration techniques are used to localize the target, the localizing error is still affected by the range measurement error as well as the errors caused by spatial distribution of sensor nodes. Thus, the Kalman filter is proposed to further reduce the effect of these errors on the estimated position of the target, and a diffusion strategy is developed to pass the knowledge of the target in association with its moving trajectory.

The rest of the chapter is organized as follows: In subsection 3.2, we formulate the problem. The trilateration uncertainty is mathematically derived in subsection 3.3. The sensor selection algorithm is discussed in subsection 3.5. The numerical analysis is presented in subsection 3.6.

3.2 Problem Formulation

The problem is formulated similar to the development in subsection 2.1 At time k, the dynamic of the tracking system is given by the following equations:

$$x_{k+1} = f(x_k, w_k) \tag{3.1}$$

$$y_{k+1} = h(x_k, \mu_k) \tag{3.2}$$

where,

– $x_k \in \mathbb{R}^6$: the state of the target,

– $w_k \sim \mathcal{N}(0, Q_k)$: the process noise with covariance matrix Q_k,

– μ_k: the noise measurement process,

– f: the state equation, and

– h: the measurement equation.

3.2.1 Measurement Model and Trilateration Algorithm

The measurement model is given by the following equation

$$d_i = \|c_i - T_k\|_2 + \mu_i, \tag{3.3}$$

where $\|.\|_2$ is standard Euclidean norm.

- $c_i \in \mathbb{R}^3$: the position of i^{th} sensor,
- $T_k \in \mathbb{R}^3$: the position of the target,
- $d_i \in \mathbb{R}$: the measurement, and
- $\mu_i \sim \mathcal{N}(0, \sigma_V^2)$: the noise measurement.

Assume that n_k sensors can sense the target, resulting in n_k nonlinear measurement equations (3.3). For each pair of integers (i, j), $1 \leq i \neq j \leq n_k$, the i^{th} and j^{th} equations in (3.3) are squared and subtracted to represent measurement in the following form:

$$A_k T_k = r_k \tag{3.4}$$

where $A_k \in \mathbb{R}^{M\times 3}$, $M = \frac{n_k(n_k-1)}{2}$, and $r_k \in \mathbb{R}^{M\times 1}$. $A_k = [A_{k_1} A_{k_2} \dots A_{k_M}]^T$ and $r_k = [r_{k_1} r_{k_2} \dots r_{k_M}]^T$.

$$A_{k_t} = 2(c_i - c_j)$$

$$r_{k_t} = (d_i - \mu_i)^2 - (\|c_i\|_2 - (d_j - \mu_j)^2 + (\|c_j\|_2$$

where $t = \varphi(i,j)$. The map $\varphi: [1 \div n_k] \times [1 \div n_k] \mapsto [1 \div M]$ is one-to-one.

The least square solution of (3.4) is given by

$$y_k = T_k = (A_k^T A_k)^{-1} A_k^T r_k. \tag{3.5}$$

The measurement equation (3.5) can be linearized as

$$y_k = H_k x_k + \theta_k \tag{3.6}$$

- $y_k \in \mathbb{R}^3$: the measured position of the target, and
- $\theta_k \in \mathbb{R}^3$: the trilateration uncertainty with covariance matrix $\Theta_k \in \mathbb{R}^{3\times 3}$.

The relationship between θ_k and μ_k is described by (3.3), (3.4), (3.5) and (3.6). The measurement matrix H_k is given by

$$H_k = \begin{bmatrix} 0 & 0 & 0 & 1 & 0 & 0 \\ 0 & 0 & 0 & 0 & 1 & 0 \\ 0 & 0 & 0 & 0 & 0 & 1 \end{bmatrix}.$$

Since matrix H_k is constant, from now on the subscript k is dropped for simpler notation $H = H_k$.

3.2.2 Trilateration Uncertainty, Sensor Selection Algorithm, and Kalman Filters.

In this chapter, we will find the solutions for the following four problems:

Problem 3.1: Determine the characteristic of the trilateration uncertainty θ_k or its covariance matrix Θ_k when n_k sensors are used in the trilateration algorithm (3.6).

Problem 3.2: Determine the relationship between Θ_k and the spatial distribution of sensor nodes.

Problem 3.3: Select a subset of n_k sensors that results in minimum trilateration uncertainty i.e., to minimize $Trace(\Theta_k)$.

Problem 3.4: Implement the distributed Kalman filter for further improving tracking quality in a distributed sense.

The solutions for problem 3.1 and 3.2 will be presented in subsection 3.3, and solution for problem 3.3 will be in subsection 3.4. The Kalman filter is implemented in a distributed sense similar to the method proposed in previous chapter.

3.3 Trilateration uncertainty

In this subsection, we derive the formula of the trilateration uncertainty matrix Θ_k in equation (3.6) for: the two-dimensional case, where two and three sensors are used to track the target; for three-dimensional case, where four sensors are used. Moreover, the formula of Θ_k will be generalized in three-dimensional coordinate system with a large number of sensor nodes. It is assumed that the range measurement is large in comparison with the measurement error.

The relationship between minimum covariance matrix i.e., $Trace\ (\Theta_k)$ and the spatial distribution of sensor nodes will be discussed.

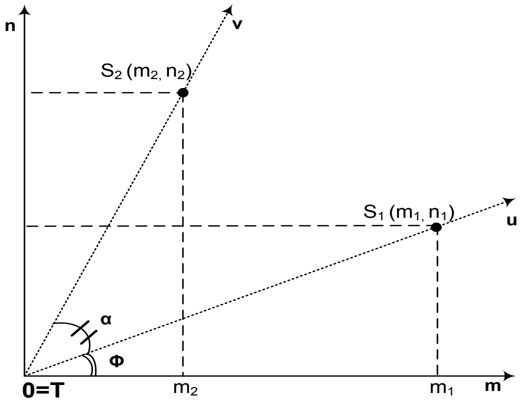

Figure 3.1: Coordinates of two sensors and the target

3.3.1 Uncertainty in Two Dimensions

Let the coordinates of the target T be $[0, 0]$ in the two-dimensional Cartesian coordinate system represented by Omn shown in Figure 3.1. Let coordinates of two sensor nodes S_1, S_2 be $[m_1, n_1]$ and $[m_2, n_2]$ respectively. The range measurement errors of sensors S_1 and S_2 are random variable u and v respectively, $u, v \sim \mathcal{N}(0, \sigma_\Lambda^2)$. The joint probability density function of two random variables (u, v) is given by

$$f_{uv}(u, v) = \frac{1}{\sqrt{2\pi\sigma_\Lambda^2}} e^{-\frac{u^2}{2\sigma_\Lambda^2}} \frac{1}{\sqrt{2\pi\sigma_\Lambda^2}} e^{-\frac{v^2}{2\sigma_\Lambda^2}} = \frac{1}{2\pi\sigma_\Lambda^2} e^{-\frac{u^2+v^2}{2\sigma_\Lambda^2}}. \qquad (3.7)$$

Theorem 3.1: If the distance from the sensor nodes S_1, S_2 to the target T are sufficiently large and let the angle $\widehat{S_1 T S_2} = \alpha$, then the covariance matrix with respect to two random variables m and n in the Cartesian coordinates $0mn$ is

$$\Theta_{mn} = \frac{\sigma_\Lambda^2}{\sin^2 \alpha} \begin{bmatrix} 1 & \cos \alpha \\ \cos \alpha & 1 \end{bmatrix}. \qquad (3.8)$$

Proof: In Cartesian coordinates $0mn$, we have

$$u = \sqrt{(m_1 - m)^2 + (n_1 - n)^2} - \sqrt{m_1^2 + n_1^2}$$

$$v = \sqrt{(m_2 - m)^2 + (n_2 - n)^2} - \sqrt{m_2^2 + n_2^2}$$

Suppose that u, v, m and n are relatively small with respect to the distance from the sensors to the target $d_1 = OS_1 = \sqrt{m_1^2 + n_1^2}$ and $d_2 = OS_2 = \sqrt{m_2^2 + n_2^2}$, we have

$$u = -m cos\varphi - n sin\ \varphi$$

$$v = -m cos(\alpha + \varphi) - n sin(\alpha + \varphi).$$

Where φ the angle between two is vectors $(\vec{m}\,,\vec{u}\,)$ and α is the angle between two vectors $(\vec{u}\,,\vec{v}\,)$ as shown in Figure 3.1.

$$u = \sqrt{(m_1 - m)^2 + (n_1 - n)^2} - \sqrt{m_1^2 + n_1^2} = \frac{-2mm_1 - 2nn_1 + m^2 + n^2}{\sqrt{(m_1 - m)^2 + (n_1 - n)^2} + \sqrt{m_1^2 + n_1^2}}$$

Since $m \ll m_1$ and $n \ll n_1$, $m_1 - m \cong m$, $n_1 - n \cong n$, and $\frac{m^2+n^2}{\sqrt{m_1^2+n_1^2}} \cong 0$, then

$$u = \frac{-2mm_1 - 2nn_1 + m^2 + n^2}{\sqrt{(m_1 - m)^2 + (n_1 - n)^2} + \sqrt{m_1^2 + n_1^2}} = -m\frac{m_1}{\sqrt{m_1^2 + n_1^2}} - n\frac{n_1}{\sqrt{m_1^2 + n_1^2}}$$

From Figure 3.2, $\cos\varphi = \frac{m_1}{\sqrt{m_1^2+n_1^2}}$ and $\sin\varphi = \frac{n_1}{\sqrt{m_1^2+n_1^2}}$. Thus, $u = -m\cos\varphi - n\sin\varphi$.

The transformation from coordinates $(\vec{u}\,,\vec{v}\,)$ to $(\vec{m}\,,\vec{n}\,)$ is given by following matrix:

$$A = -\begin{bmatrix} \cos\varphi & \cos(\alpha+\varphi) \\ \sin\varphi & \sin(\alpha+\varphi) \end{bmatrix}.$$

Since $\det(A) = \sin\alpha$, the probability density function with respect to random variables (m, n) is

$$f_{mn}(m,n) = \frac{1}{2\pi\sigma_\Lambda^2}\frac{1}{\sin\alpha}e^{-\frac{1}{2\sigma_\Lambda^2}[(u\,cos\,\varphi+v\,cos(\alpha+\varphi))^2+((u\,sin\,\varphi+v\,sin(\alpha+\varphi))^2]}$$

$$= \frac{1}{2\pi\sigma_\Lambda^2}\frac{1}{\sin\alpha}e^{-\frac{m^2+2mn\,cos\,\alpha+n^2}{2\sigma_\Lambda^2}}$$

Thus, the covariance matrix with respect to coordinates (m,n) is

$$\Theta_{mn} = \frac{\sigma_\Lambda^2}{\sin^2\alpha}\begin{bmatrix} 1 & \cos\alpha \\ \cos\alpha & 1 \end{bmatrix}. \blacksquare$$

Remark 3.1: The covariance matrix Θ_{mn} depends only on the angle formed by the two sensors and the target, and the measurement variance of each sensor. Since Θ_{mn} does not depend on the angle φ, it is constant as long as two vectors $\vec{m}$ and $\vec{n}$ are perpendicular.

Two eigenvalues of Θ_{mn} are λ_1 and λ_2, and $\lambda_1 + \lambda_2 = \frac{2\sigma_\Lambda^2}{sin^2\,\alpha} \geq 2\sigma_\Lambda^2$. The equality holds when $\sin\alpha = 1$. Thus, when the two sensors and the target form a right triangle, the measurement uncertainty is minimized.

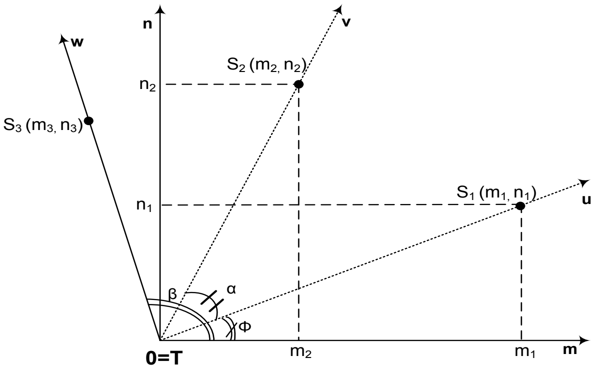

Figure 3.2: Coordinates of three sensors and the target

Theorem 3.2: Given three sensor nodes S_1, S_2, S_3, and the target T at the origin, the angles $\widehat{S_1 T\, S_2} = \alpha,\ \ \widehat{S_2 T\, S_3} = \beta$. Suppose that the distance from each sensor to the target is sufficiently large. The noise covariance matrix of the target in the Cartesian coordinates $0mn$ is.

$$\Theta_{mn} = \frac{\sigma_\Lambda^2}{\sin^2\alpha}\begin{bmatrix} 2-\cos^2(\alpha-\beta) & 2\cos\alpha - \cos\beta\ \cos(\beta-\alpha) \\ 2\cos\alpha - \cos\beta\ \cos(\beta-\alpha) & 2-\cos^2\beta \end{bmatrix} \quad (3.9)$$

Proof: In order to transform the probability density function (pdf) of three random variables $u,\ v$, and w to the pdf of two random variable m, and n, we introduce a dummy variable $l = w$. The transformation matrix is given by:

$$\begin{bmatrix} u \\ v \\ w \end{bmatrix} = -B \begin{bmatrix} m \\ n \\ l \end{bmatrix}$$

where

$$\mathrm{B} = \begin{bmatrix} \cos\varphi & \cos(\alpha+\varphi) & \cos(\beta+\varphi) \\ \sin\varphi & \sin(\alpha+\varphi) & \cos(\beta+\varphi) \\ 0 & 0 & 1 \end{bmatrix}.$$

We have

$$f_{uvw}(u,v,w) = (\frac{1}{\sqrt{2\pi\sigma_\Lambda^2}})^3 e^{-\frac{u^2+v^2+w^2}{2\sigma_\Lambda^2}}.$$

Since $\det(B) = \sin\alpha$, and

$$u^2 + v^2 + w^2 = q(m,n,l)$$

$$= m^2 + n^2 + 2l^2 + 2mn\cos\alpha + 2mn\cos(\alpha-\beta) + 2ml\cos\beta.$$

The pdf of three random variables $m, n,$ and o is given by

$$f_{mno}(m,n,l) = (\frac{1}{\sqrt{2\pi\sigma_\Lambda^2}})^3 \frac{1}{\sin\alpha} e^{-\frac{q(m,n,l)}{2\sigma_\Lambda^2}}.$$

The pdf of two random variables m, and n is the marginal pdf of $m, n,$ and o

$$f_{mn}(m,n) = \int_{0=-\infty}^{o=+\infty} (\frac{1}{\sqrt{2\pi\sigma_\Lambda^2}})^3 \frac{1}{\sin\alpha} e^{-\frac{q(m,n,l)}{2\sigma_\Lambda^2}} dl$$

$$= \frac{1}{2\pi\sigma_\Lambda^2} \frac{1}{2\sin\alpha} e^{-\frac{1}{2\sigma_\Lambda^2}[m^2(2-cos^2(\alpha-\beta))+2mn(2\cos\alpha-\cos\beta\ \cos(\beta-\alpha))+n^2(2-cos^2\beta)]}$$

From the joint Gaussian distribution property of the above pdf equation, the covariance matrix of two random variables m and n can be easily derived. ■

Remark 3.2: The two eigenvalues of Θ_{mn} are λ_1 and λ_2, and the total variance in two directions m and n is:

$$\begin{aligned} Sm = Trace(\Theta_{mn}) = \lambda_1 + \lambda_2 = \sigma_m^2 + \sigma_n^2 \\ = \frac{\sigma_\Lambda^2}{sin^2 \alpha}[4 - cos^2 \beta - cos^2(\alpha - \beta)] \end{aligned} \tag{3.10}$$

Corollary 3.3: Given a constant α such that $0° < \alpha < \pi$, the total variance Sm is minimized when

$$\left[\begin{aligned} \beta = \frac{\alpha}{2} + k\pi \text{ if } 0 < \alpha < \frac{\pi}{2} \\ \beta = \frac{\alpha}{2} + \frac{\pi}{2} + k\pi \text{ if } \frac{\pi}{2} < \alpha < \pi \end{aligned} \right. \tag{3.11}$$

where k is an integer.

Proof: $Sm = \lambda_1 + \lambda_2 = \sigma_m^2 + \sigma_n^2 = \frac{\sigma_\Lambda^2}{\sin^2 \alpha}[4 - \cos^2 \beta - \cos^2(\alpha - \beta)]$

$$= \frac{\sigma_\Lambda^2}{\sin^2 \alpha}\left[3 - \frac{1}{2}[\cos 2\alpha + \cos(2\beta - 2\alpha)\right] = \frac{\sigma_\Lambda^2}{\sin^2 \alpha}[3 - \cos \alpha \cos(2\beta - \alpha)]$$

Since α is constant, and $1 \geq \cos(2\beta - \alpha) \geq -1$

$$\frac{\sigma_\Lambda^2}{\sin^2 \alpha}(3 - |\cos \alpha|) \leq Sm \leq \frac{\sigma_\Lambda^2}{\sin^2 \alpha}(3 + |\cos \alpha|)$$

Thus, if $\cos \alpha > 0$ or $0 \leq \alpha < \frac{\pi}{2}$, then

$Sm = \min_{\beta \in [0,\pi]} Sm = \frac{\sigma_\Lambda^2}{\sin^2 \alpha}(3 - \cos \alpha)$ when $\cos(2\beta - \alpha) = 1$ or $\beta = \frac{\alpha}{2} + k\pi$ where k is an integer.

If $\cos \alpha < 0$ or $\frac{\pi}{2} < \alpha \leq \pi$, then

$Sm = \min_{\beta \in [0,\pi]} Sm = \frac{\sigma_\Lambda^2}{\sin^2 \alpha}(3 + \cos \alpha)$ when $\cos(2\beta - \alpha) = -1$ or $\beta = \frac{\alpha}{2} + \frac{\pi}{2} + k\pi$. ■

3.3.2 *Uncertainty in Three Dimensions*

We now consider the three-dimensional (3D) case. Suppose that the coordinates of the target are $(0, 0, 0)$ in the Cartesian coordinate system represented by $0mno$. The coordinates of three sensor nodes S_1, S_2, and S_3 are $(m_1, 0, 0)$, $(m_2,\ n_2,\ 0)$, and $(m_3,\ n_3,\ o_3)$ respectively. $H = \ (m_3,\ n_3,\ 0)$ is the projection of S_3 onto the plane 0mn. Furthermore, let $\widehat{S_1TS}_2 = \alpha$, $(S_1T,\ S_3TH) = \beta$, and $(S_3T,\ S_1TS_2) = \gamma$ where β is the angle between S_1T and the plane S_3TH and γ is the angle between S_3T and the plane S_1TS_2 as shown in Figure 3.2.

Theorem 3.4: Suppose the distances from the sensor nodes S_1, S_2, S_3 to the target are sufficiently large, Then, the sum variance with respect to three random variables m, n, and o depends only on γ but not β, and is minimized when $\gamma = 90°$.

Since $To \perp S_1TS_2$, the uncertainty in the To axis depends on the uncertainty in TS_3 and TH directions. By Theorem 3.1, this value is minimized when $\gamma = \widehat{HTS_3} = 90°$.■

3.3.3 *Uncertainty of Trilateration Algorithm*

The least square solution of equation (3.5) is

$$y_k = p_k = (A_k^T A_k)^{-1} A_k^T r_k. \tag{3.12}$$

Thus, the trilateration uncertainty is the measurement covariance matrix given by

$$\Theta_k = E\{y_k y_k^T\} = (A_k^T A_k)^{-1} A_k^T \Phi_k A_k [(A_k^T A_k)^{-1}]^T \tag{3.13}$$

where $\Phi_k = E\{r_k r_k^T\}$.

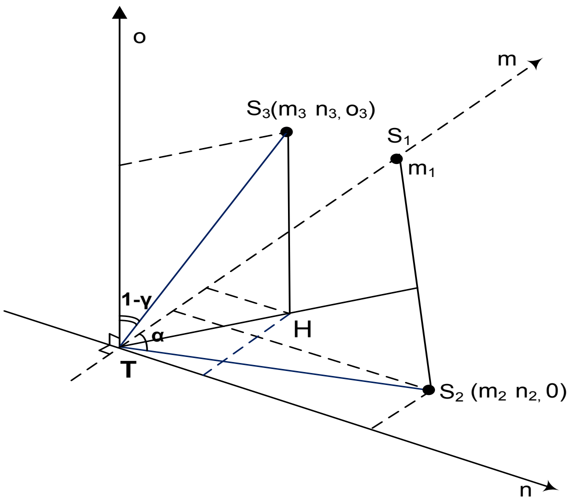

Figure 3.3: Trilateration uncertainty by three sensors

Theorem 3.5: The measurement covariance matrix Θ_k given in (3.13) is uniformly bounded.

Proof: Since matrix A_k is deterministic, it is sufficient to prove the matrix Θ_k is uniformly bounded in the sense that $\mathrm{Trace}(\Theta_k) \leq B < \infty$. Without loss of generality, suppose that the target is at the origin. Let φ be a one on one mapping $\varphi\colon [1 \div M] \mapsto [1 \div n_k] \times [1 \div n_k]$, $t = \varphi(i,j)$, and $M = \frac{1}{2} n_k(n_k - 1)$. Thus, for each element t, $1 \leq t \leq M \; of \; r_k = [\, r_{k1} \quad r_{k2} \quad \cdots \quad r_{kM}]^T$, from (3.13) we have:

$$E\{r_{kt}^2\} = E\{(-2d_i\mu_i + \mu_i^2 + 2d_j\mu_j - \mu_j^2)^2\}$$

$$= (4d_i^2 + E\{\mu_i^2\})E\{\mu_i^2\} + \left(4d_j^2 + E\{\mu_j^2\}\right)E\{\mu_j^2\}$$

$$= \left(4d_i^2 + 4d_j^2\right)\sigma_\Lambda^2 = \sigma_1 \text{ where}$$

$$E\{\mu_i\} = 0;\; E\{\mu_i^2\} = \sigma_\Lambda^2.$$

$$E\{r_{kt}^2\} = \sigma_1 \tag{3.14}$$

where and $1 \leq i \neq j \leq n_k$.

Now, suppose $t_1 = \varphi(i,j)$ and $t_2 = \varphi(i,l)$ where $1 \le i,\ j \le n_k$ and j$\neq\ i \neq\ l$. Thus, $E\{r_{t_1}r_{t_2}\} = E\{(-2d_i\mu_i + \mu_i^2 + 2d_j\mu_j - \mu_j^2)(-2d_i\mu_i + \mu_i^2 + 2d_l\mu_l - \mu_l^2)\}$

$$= 4d_i^2\sigma_\Lambda^2 = \sigma_2$$

$$E\{r_{kt}^2\} = \sigma_2 \qquad (3.15)$$

If $t_3 = \varphi(i,j)$ and $t_4 = \varphi(l,m)$, then $E\{r_{t_3}r_{t_4}\} = 0$.

Thus, the diagonal elements of matrix Φ_k in (3.13) are σ_1, some of the elements are σ_2 (equation (3.15)), and all the other elements are zero. Since matrix A_k is full rank and deterministic, from (3.13) Θ_k is bounded.

3.4 Sensor Selection Algorithm

In this subsection, an algorithm is proposed to choose three and four sensor nodes that minimize trilateration uncertainty. At each step, the algorithm does not need to calculate the trilateration uncertainty matrix Θ_k, but it exploits the relationship between spatial distribution of sensor nodes and Θ_k; which results in significant reduction in required computational power. The input of the algorithm includes n_k sensor nodes within the measurement range of the target, their coordinates, and the estimate coordinates of the target. Meanwhile, the algorithm determines four sensors and their coordinates.

The flowing pseudo code is used to select three sensor nodes in two-dimensional case.

```
Function-2D($n_k$; $C$; $T_e$)
 Step 1.   Let $\widehat{S_iT_eS_j} = \alpha$
 Step 2.   Choose $i$, $j$ such that $|\cos(\alpha)|$ is minimized
 Step 3.    For each $k$, let $\widehat{S_\imath T_e S_k} = \beta$
 Step 4.    Choose $k$ such that
             i.  $\cos(2\beta - \alpha)$ is maximized when $0 \leq \alpha < \frac{\pi}{2}$
            ii.  $\cos(2\beta - \alpha)$ is minimized when $\frac{\pi}{2} \leq \alpha < \pi$
 Return ($i$, $j$, $k$)
```

- n_k is the number of neighbor sensor nodes.
- $\mathcal{C}$=[S_1.. S_{n_k}] are the coordinates of n_k sensor nodes.
- T_e is the estimated position of target.
- S_i, S_j, and S_k are positions of sensors i, j, and k.

Theorem 3.6: The Function-2D yields the suboptimal solution that minimizes the trilateration uncertainty i.e., $Trace\ (\Theta_k)$.

Proof: By Theorem 3.1 and Remark 3.1, sensors S_i and S_j in step 2 are the best choice. By Theorem 3.2 and Corollary 3.3, the selection of S_k in step 4 minimizes Trace (Θ_k).

The total number of calculations are:

$$\frac{n_k(n_k-1)}{2} + (n_k - 2) = \frac{n_k(n_k+1)}{2} - 2. \qquad (3.16)$$

The complexity of the Function-2D is equivalent to $O(n_k^2)$ which is much smaller than $\binom{3}{n_k}$ of $O(n_k^3)$ when exhaustive search is used.

The flowing pseudo code is used to select three sensor nodes in three-dimensional case.

```
Function-3D($n_k$; $\mathcal{C}$; $T_e$)
```

```
Step 1.   Choose $i$, $j$ such that $\left|\cos(\widehat{S_iT_eS_j})\right|$ is minimized
Step 2.   Choose $k$ such that $\left|\cos(S_kT_e\,, S_iT_eS_j\,)\right|$ is minimized
Step 3.   Choose $l$ such that $Trace(\Theta_k)$ is minimized
Return ($i$, $j$, $k$, $l$)
```

- n_k is the number of neighbor sensor nodes.
- $\mathcal{C}$=[S_1.. S_{n_k}] are the coordinates of n_k sensor nodes..
- T_e is the estimated position of target.
- S_i, S_j, S_k, and S_l are positions of sensor i, j, k, and l.
- $(S_kT_e\,, S_iT_eS_j)$ in step 2 is the angle between line S_kT_e and plane $S_iT_eS_j$.
- Matrix Θ_k is given by (3.13) where four selected sensors are S_i, S_j, S_k, and S_l.

Theorem 3.7: The Function-3D yields the suboptimal solution that minimizes the trilateration uncertainty, i.e., $Trace\ (\Theta_k)$.

Proof: By Theorem 3.1 and Remark 3.1, sensors S_i and S_j in step 1 are the best choice. By Theorem 3.4, the selection of S_k sensor minimizes the trilateration uncertainty.

The total number of calculations are:

$$\frac{n_k(n_k-1)}{2} + (n_k - 2) + (n_k - 3) = \frac{n_k(n_k+3)}{2} - 5. \tag{3.17}$$

The complexity of the Function-3D is equivalent to $O(n_k^2)$ which is much smaller than $\binom{4}{n_k}$ of $O(n_k^4)$ when exhaustive search is used.

3.5 Discussion

3.5.1 Convergence of the Kalman Filter

The convergence analysis of the Kaman filter is proved in a similar fashion in Section 2.3. The noise measurement covariance matrix Θ_k, in this Chapter, varies for each tracking interval while Θ_k is assumed to be constant in Chapter 2. However, the proof is still valid.

3.5.2 *Effect of Nonlinear System*

The conditions for the stability of the Kalman filter in equations (2.21), (2.22) are necessary, but not sufficient. When the Kalman filter converges, the error covariance matrix P_{k+1} is expected to converge to a constant closed to zero, the condition $HP_{k+1}H^T - \Theta_k \leq 0$ will be met easily. The second condition in (2.22) depends on the nonlinearity of the system. If the system is highly nonlinear (i.e., $\lambda_{max}(a_k)$ is large), the second condition does not hold. However, according to the proof of stability in Section 2.3.2, we cannot conclude the Kalman filter is unstable. Thus, the assumptions in Section 2.2.1 guarantee the convergence of the extended Kalman filter.

3.6 Numerical Example

In this section, we first demonstrate the importance of the relationship between trilateration uncertainty and spatial distribution of sensor nodes.

In Figure 3.4a, six sensor nodes were deployed in an area of dimension 3.5×3 unit and the movement of the target is represented by a solid line. The coordinates of six nodes were given in Table 3.1. In Figure 3.4b, the trilateration uncertainty of all six nodes was generally small than that of three sensors (#1, #2, #3). The trilateration uncertainty varied according to the relative location of the target and sensor nodes, and was smallest when the coordinate of the target (in x-direction) is about 0.9, where the target was close to the center of three nodes (#1, #2, #3). Moreover despite the error in the location of the target, the trilateration uncertainty could be estimated as it varied smoothly according to the target trajectory. In Figure 3.4c, the trilateration uncertainty, when five nodes (#1, #2, #4, #5, #6) were used was much bigger than the trilateration uncertainty of two cases in Figure 3.4b. These five nodes were almost collinear. In this case, the selection algorithm should choose the three node (#1, #2, #3) configuration over these five node one.

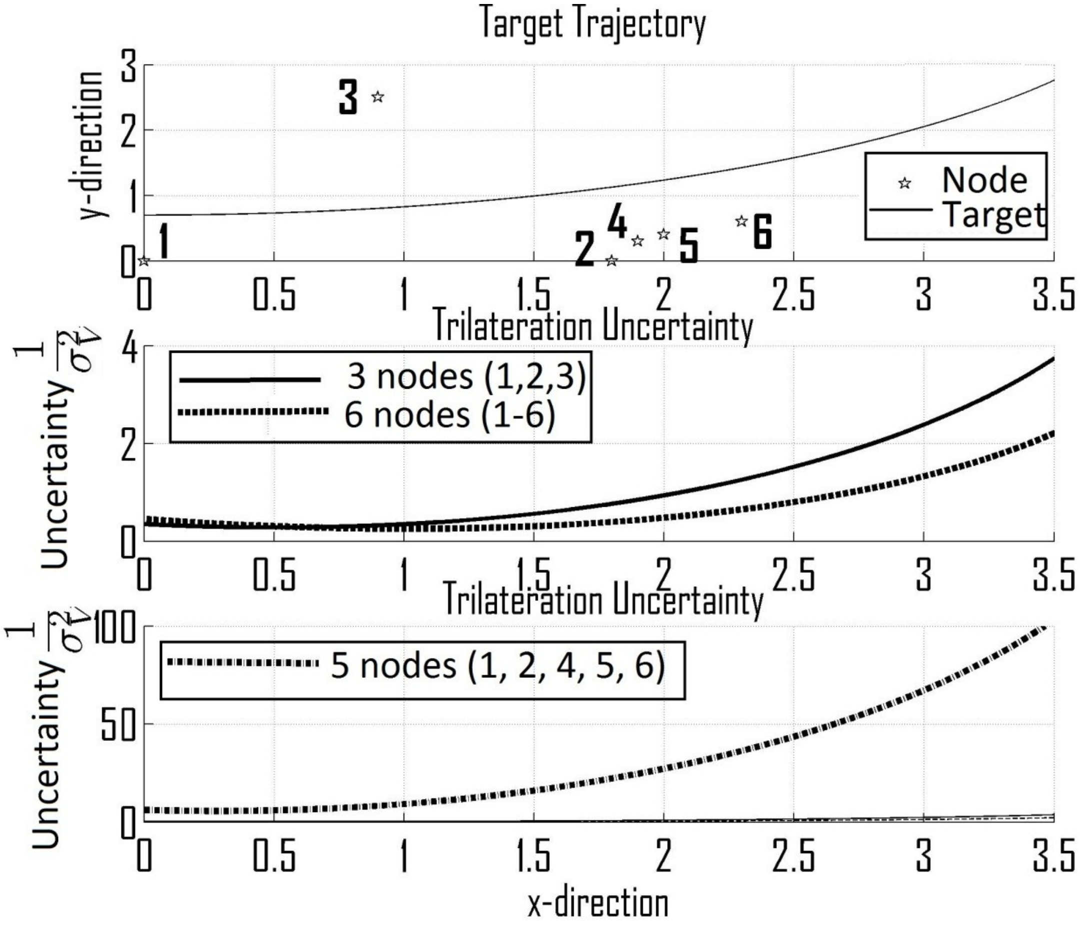

Figure 3.4: Sensor distribution and trilateration uncertainty

Table 3.1: Coordinates of sensor nodes

Sensor node	x-direction	y-direction
1	0	0
2	1.8	0
3	0.9	2.5
4	1.9	0.3
5	2.0	0.4
6	2.3	0.6

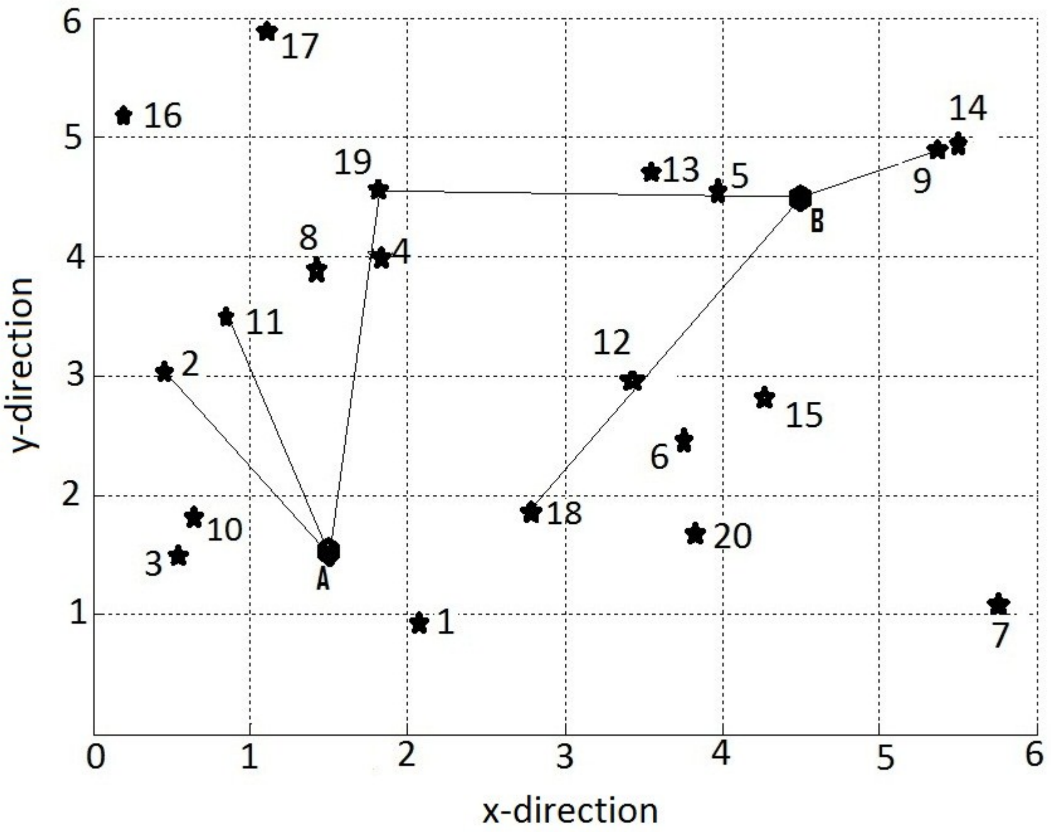

Figure 3.5: Selection of three sensor nodes

In Figure 3.5, 20 sensor nodes were randomly deployed, and the sensing radius was 4.0 units. When the target was at the location A, three sensors #2, #11, and #19 result in smallest trilateration uncertainty. When the target was at the location B, three sensors #14, #18, and #19 were the best selection. Coincidently, the sensor node #19 appeared in both case.

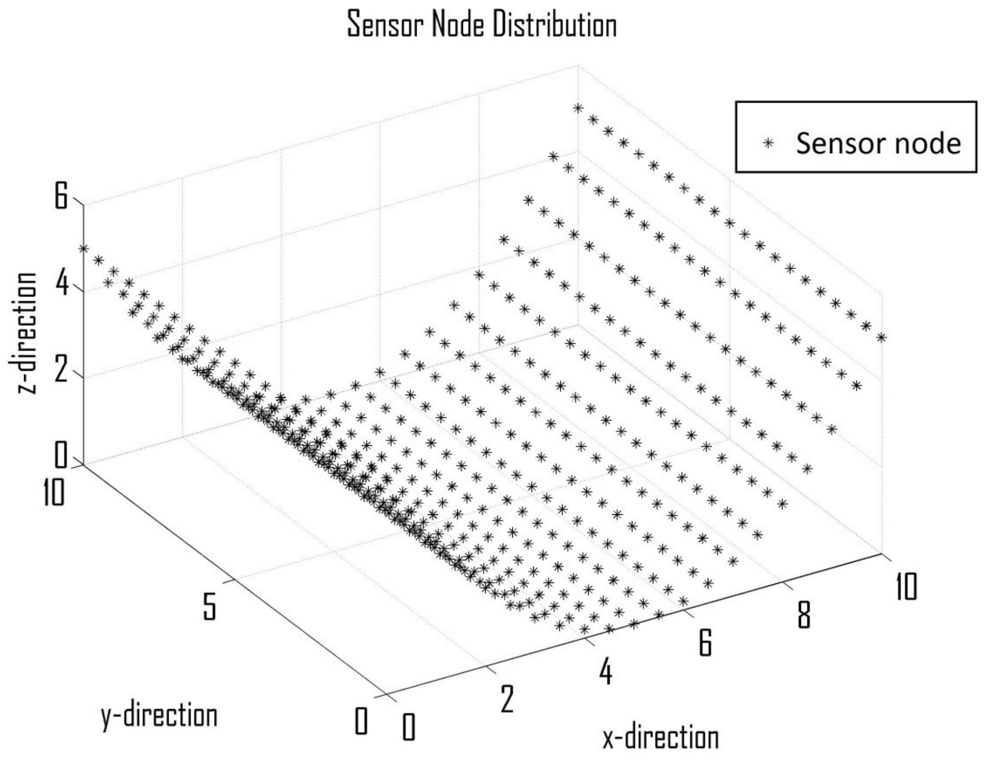

Figure 3.6: Moving trajectory of the target and distribution of sensor nodes

We now demonstrate the sensor selection algorithm and implementation of the Kalman filter for tracking targets in 3D. The sensor field is assumed to be a cube of the dimension $10 \times 10 \times 6$ units. Assume that 441 sensor nodes are uniformly distributed along a 3D parabolic surface. The target is assumed to move with a sinusoidal velocity profile in x and y-direction, while it moved in parabolic profile in z-direction at 0.5 unit above the sensor field, as shown in Figure 3.6. The power consumption profile is based on the analysis in subsection 2.6.2.

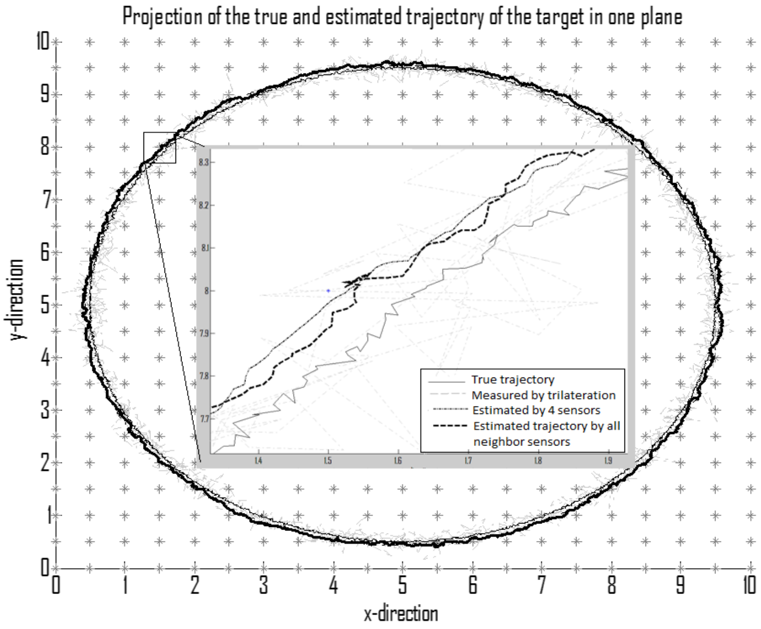

Figure 3.7: True and estimated trajectory of the target and distribution of the sensor nodes. Estimation error is smaller when more sensor nodes are used for tracking. Four sensor nodes used for tracking were selected based on the algorithm given in Theorem 3.7**.** Tracking error is greatly reduced using Kalman filter.

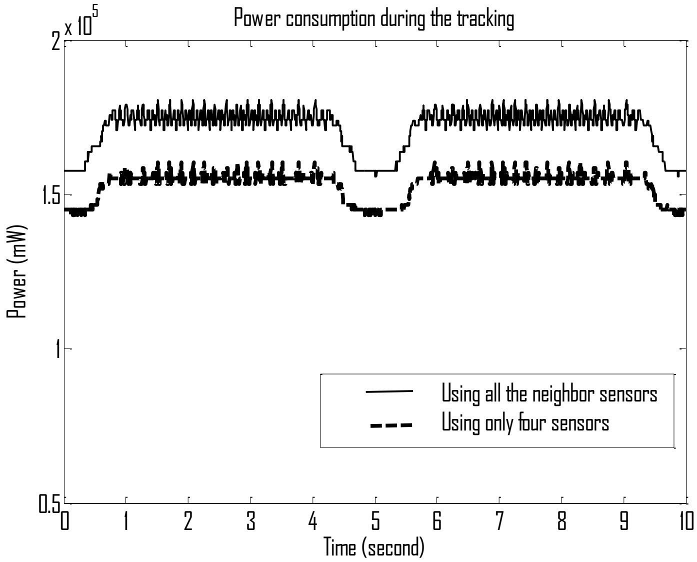

Figure 3.8: Power consumption of the sensor network during the tracking.

3.7 Conclusion

This chapter addressed the trilateration uncertainty during the tracking of dynamic targets using a Wireless Sensor Network. The relationship between the trilateration uncertainty and the location of the sensor nodes can be exploited during the selection of the nodes to track a target. The tracking performance was further improved by implementing the Kalman filter. Moreover, the proposed algorithm reduces both the computational cost and the total power consumption in the network compared to similar algorithms reported in literature. The numerical simulations demonstrated the flexibility and power of the proposed tracking algorithm.

Chapter 4

Mobile Robot Assisted Target Tracking

Target tracking using Wireless Sensor Networks (WSNs) is a widely studied application area. However, the available power at each sensor node and the energy required to transmit the sensed information to a network sink have limited the use of WSNs in target tracking applications. In this chapter, we study the use of a mobile robot, working in conjunction with the WSN, to track a target. The trilateration approach from Chapter 2 and 3 is used to detect the presence of the target and a Kalman filter is used to estimate its location. An algorithm is proposed that enables the selection of a minimum number of sensor nodes to track the target and to determine the path of the mobile robot for efficient tracking. Theoretical proofs are developed to mathematically demonstrate the convergence of the target tracking algorithm.

4.1 Introduction

Target tracking using Wireless Sensor Networks (WSNs) is a widely studied application area. However, tracking of targets using WSNs poses several challenges. The first challenge is the selection of a set of sensor nodes [82, 83] within the measurement range of the target that results in the smallest bias in estimation. Due to the effect of geometric dilution of precision [93, 94], a set of small sensor nodes can improve the accuracy of the estimation while a large number of sensor nodes can result in significant localization errors. Once the required nodes are determined, the second challenge is to determine the uncertainty of the trilateration algorithm [83, 95, 96] and to further reduce localization errors. Moreover, the implementation of complex tracking algorithms is difficult due to the low computational capability of the nodes. In a large scale sensor network, the tracking algorithm should be implemented in a distributed fashion [84]. In such distributed implementations, the handing over of knowledge of the target from one master node to the subsequent one is another challenge to be addressed. Further, the estimated data has to be transmitted to the sink, a process that requires significant power and bandwidth allocation. Extending the useful life of WSNs by reducing the overall power consumption is another challenge that has to be addressed [31, 88].

The use of mobile robots in surveillance, perimeter patrol, and target tracking applications has also been widely studied [78]. Motion planning of nonholonomic mobile robot was presented [79, 80]. Coordinated control of mobile robots was addressed by Jung and Sukhatme in [81]. However, determining the location of a target using one mobile node is not an easy task. The use of mobile robots in conjunction with WSN can address this problem.

In this chapter, we propose a novel method for solving the above challenges by using a mobile robot to assist sensor nodes to track the target. The mobile robot uses the range measurements from the active nodes and executes the trilateration algorithm to determine the location of the target, and implements a Kalman filter to further reduce the tracking error. The mobile robot is assumed to move freely around the sensor field. Based on the estimated trajectory of the target and its current position, the mobile robot plans selects a trajectory that minimizes the total distance traveled. In contrast to Chapters 2 and 3, this approach eliminates the need (1) to hand-over between leader nodes and (2) to communicate with the network sink. Numerical simulations and mathematical analysis verify the effectiveness of the proposed method in reducing error in the estimated location of the target. The planning strategy also minimizes the path of the mobile robot.

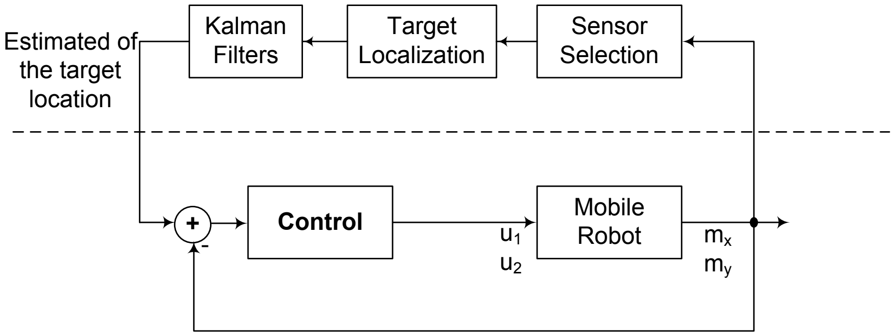

Figure 4.1: System overview

4.2 Problem Formulation

The tracking of the target is accomplished by a ground based mobile robot. The robot follows the trajectory of the target on the ground and is within one-hop communication of the sensor nodes in the neighborhood of the target. The mobile robot selects a set of sensor nodes to measure the distances to the target and to transmit these distances to the mobile robot. The mobile robot then runs the trilateration algorithm to localize the coordinates of the target and executes the Kalman filter for further noise reduction. The following assumptions are made for the theoretical development in this chapter: (1) Mobile robot has the necessary computational capability to determine its location by range measurements from sensors and, (2) the mobile robot can move freely in the sensor field.

4.2.1 Tracking System

The settings of the problem are similar to the one given in subsection 3.2. We consider the tracking problem for only 2D coordinate system. At time k, the dynamic of the tracking system is given by the following equations:

$$x_{k+1} = f(x_k, w_k) \tag{4.1}$$

$$x_{k+1} = f(x_k, w_k) \tag{4.2}$$

where

- $x_k \in \mathbb{R}^4$: the state of the target,
- $w_k \sim \mathcal{N}(0, Q_k)$: the process noise with covariance matrix Q_k,
- μ_k: the measurement noise,
- f: the state equation, and
- h: the measurement equation.

4.2.2 Measurement Model and Trilateration Algorithm

The measurement model is given by the following equation

$$d_i = \|c_i - T_k\|_2 + \mu_i, \tag{4.3}$$

where $\|.\|_2$ is standard Euclidean norm,

- $c_i \in \mathbb{R}^2$: the position of i^{th} sensor,
- $T_k \in \mathbb{R}^2$: the position of the target,
- $d_i \in \mathbb{R}$: the measurement, and
- $\mu_i \sim \mathcal{N}(0, \sigma_V^2)$: the noise measurement.

Assuming that n_k sensors can sense the target, resulting in n_k nonlinear measurement equations (4.3). For each pair of integers (i, j), $1 \leq i \neq j \leq n_k$, the i^{th} and j^{th} in (4.3) are squared and subtracted to represent the measurement in the following form.

$$A_k T_k = r_k \tag{4.4}$$

where $A_k \in \mathbb{R}^{M \times 2}$, $M = \frac{n_k(n_k-1)}{2}$, and $r_k \in \mathbb{R}^{M \times 1}$. $A_k = [A_{k_1} A_{k_2} \dots A_{k_M}]^T$ and $r_k = [r_{k_1} r_{k_2} \dots r_{k_M}]^T$.

$$A_{k_t} = 2(c_i - c_j),$$

$$r_{k_t} = (d_i - \mu_i)^2 - (\|c_i\|_2 - (d_j - \mu_j)^2 + \|c_j\|_2)$$

where $t = \varphi(i, j)$. The map $\varphi: [1 \div n_k] \times [1 \div n_k] \mapsto [1 \div M]$ is one-to-one.

The least square solution of trilateration algorithm in (4.4) is given by

$$y_k = T_k = (A_k^T A_k)^{-1} A_k^T r_k. \tag{4.5}$$

The measurement equation (4.5) can be linearized as

$$y_k = H_k x_k + \theta_k. \tag{4.6}$$

- $y_k \in \mathbb{R}^2$: the measured position of the target, and
- $\theta_k \in \mathbb{R}^2$: the trilateration uncertainty with covariance matrix $\Theta_k \in \mathbb{R}^{2 \times 2}$.

The relationship between θ_k and μ_k is described by (4.3), (4.4), (4.5) and (4.6). The measurement matrix H_k is given by

$$H_k = \begin{bmatrix} 0 & 0 & 1 & 0 \\ 0 & 0 & 0 & 1 \end{bmatrix}.$$

Since matrix H_k is constant, the subscript k is dropped to simplify the notation, i.e., $H = H_k$.

4.2.3 Movement of the Mobile Robot

A simplified dynamical representation of a car-like mobile robot can be expressed as

$$\begin{bmatrix} \dot{m}_x \\ \dot{m}_y \\ \dot{\omega} \end{bmatrix} = \begin{bmatrix} \cos\omega \\ \sin\omega \\ 0 \end{bmatrix} v\cos\varphi + \begin{bmatrix} 0 \\ 0 \\ 1 \end{bmatrix} v \tag{4.7}$$

where (m_x, m_y) are the coordinates of the center of the mobile robot, and ω is the orientation of the robot with respect to the East direction. Whereas, $\dot{m}_x$, $\dot{m}_y$, $\dot{\omega}$ represent their derivative counterparts. v is the speed, and φ is the steering angle of the front wheels as shown in Figure 4.2. Let V_{max} and φ_{max} be the maximum speed of the target and maximum steering angle of the mobile robot. The constraints of the system are

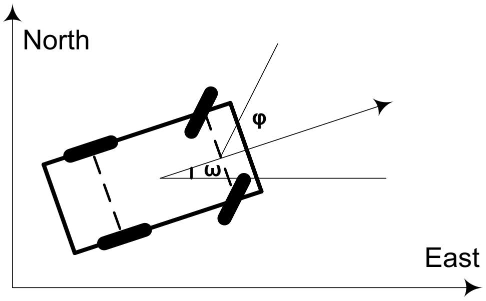

Figure 4.2: Diagram of a car-like mobile robot

$$\begin{cases} v \leq V_{max} \\ \varphi \leq \varphi_{max} \end{cases}. \tag{4.8}$$

Let $u_1 = v\cos\varphi$ and $u_2 = v\sin\varphi$. The equation (4.7) can be expressed as

$$\begin{bmatrix} \dot{m}_x \\ \dot{m}_y \\ \dot{\omega} \end{bmatrix} = \begin{bmatrix} \cos\omega \\ \sin\omega \\ 0 \end{bmatrix} u_1 + \begin{bmatrix} 0 \\ 0 \\ 1 \end{bmatrix} u_2. \tag{4.9}$$

The constraint in (4.9) becomes

$$\begin{cases} u_1 \leq V_{max} \cos \varphi_{max} \\ u_1 \tan \varphi_{max} \geq u_2 \end{cases}. \tag{4.10}$$

The control problem is to find an input u such that the mobile robot is still within one communication hop from the sensing nodes at time $k+1$ while the total traversed distance is minimized.

4.3 Movement Strategy of the Mobile Robot

Let the coordinate of the mobile robot at the time k be (m_{k1}, m_{k2}) represented by point M_k in Figure 4.3. Let the estimated position of the target be at (t_{k1}, t_{k2}) represented by point T_k, and the target heading is (h_{k1}, h_{k2}), i.e., the vector $\overrightarrow{T_k T_{k+1}}$. Let the sensing radius and communication radius be τ_S and τ_C, respectively. The uncertainty of the estimated target is $\Delta\tau_T$. In order for the mobile robot to be within one communication hop of the neighborhood of the target, the next position of the mobile robot M_{k+1} has to satisfy the following condition:

$$|M_{k+1}T_{k+1}| \leq \tau_C - (\tau_S + \Delta\tau_T) \tag{4.11}$$

Thus, $min|M_{k+1}T_{k+1}| = M_{k+1}T_{k+1} - |\tau_C - (\tau_S + \Delta\tau_T)|$. Obviously, if $M_{k+1}T_{k+1} \leq |\tau_C - (\tau_S + \Delta\tau_T)|$, the mobile robot does not require to move. In order for the mobile robot to move from point M_k to point M_{k+1}, the system (4.7) needs to be locally controllable.

Theorem 4.1: The system (4.7) of the car-like mobile robot with constraint (4.10) is locally controllable.

Theorem 4.2: There exists an optimal path from M_k to M_{k+1} which minimizes the travel distance.

The proofs of Theorem 4.1 and 4.2 are given by Laumond [80] and Reeds [97].

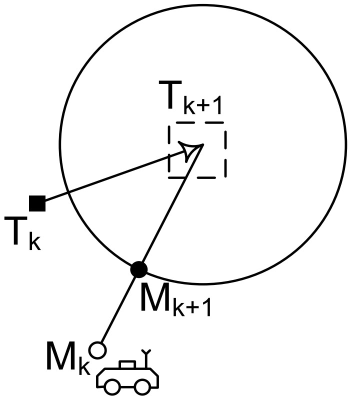

Figure 4.3: Movement of the mobile robot

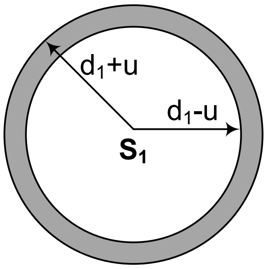

Figure 4.4: Measurement uncertainty of one sensor

Theorem 4.3: If at time t_k, the mobile robot is within one communication hop of the nodes that detect the target, the moving strategy described above guarantees that the mobile robot is within one communication hop of the target during the time t_k to t_{k+1}.

Proof: When the target moves from T_k to T_{k+1}, the mobile robot moves from M_k to M_{k+1}. Let $\Delta\Gamma = \tau_C - (\tau_S + \Delta\tau_T)$. We have $M_kT_k \leq \Delta\Gamma$ and $M_{k+1}T_{k+1} \leq \Delta\Gamma$. If $\Delta t = t_{k+1} - t_k$, (the sampling time), is sufficiently small, both the target and mobile robot move in linear trajectory. Thus, for any $t \in [t_k, t_{k+1}]$, $M_{k(t)}T_{k(t)} \leq \Delta\Gamma$.■

4.4 Trilateration Uncertainty and Sensor Selection

Suppose that the range measurement of each sensor node is subjected to white Gaussian noises $\mathcal{N}(0, \sigma_{\Lambda}^2)$. After using the trilateration method, the covariance matrix of the measurement noise of the target in Equation (4.5) is Θ_k. If n_{k} nodes can sense the target, the mobile robot has to select a set of minimum number of sensors while still maintaining the predefined tracking performance. Understanding the relationship between Θ_k and the spatial distribution of sensor nodes, a greedy algorithm can select a set of sensors that minimizes the variance of trilateration uncertainty, i.e., $Trace(\Theta_k)$.

The sensor selection algorithm bases on the greedy approach. First, the intersection criterion removes nodes whose coordinates are closed to collinear. Secondly, the selection of two sensors that gives the best trilateration performance bases on Theorem 3.1. When two sensors are chosen, the third sensor is selected according to Theorem 3.2. If more sensor nodes need to be selected for reducing trilateration uncertainty, the next selected sensor will minimize $Trace(\Theta_k)$ in Equation (4.5).

4.4.1 Intersection Criterion

Let d_1 be the distance from the sensor node S_1 to the target, and p be the probability that the target is in the donut shape of radius $d_1 - u$ and $d_1 + u$ in Figure 4.4, where $u = 2\sigma_{\Lambda}$ (σ_{Λ} is the standard deviation of the measurement noise). Let d_1 and d_2 be the distances from two sensors $S_1$and S_2 to the target, respectively; and $S_1S_1 = d$. Thus, p is the probability of the target is in either one of two darker shaded areas in Figure 4.5c, if the following conditions hold. Assume $d_1 < d_2$.

$$\begin{cases} d_1 + d_2 \geq d + 2u \\ d_1 + d \geq d_2 + 2u \end{cases} \tag{4.12}$$

The first condition in equation (4.12) avoids the case in Figure 4.5b, while the second condition guarantees that the scenario in Figure 4.5a does not happen.

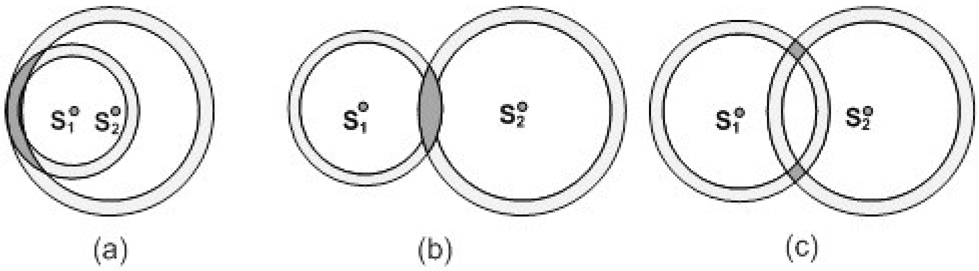

Figure 4.5: Measurement uncertainty of two sensor nodes**.** The settings in (a) and (b) result in larger uncertainty in comparison with the setting in (c) does.

4.4.2 Angle Criterion and Choice of Two Sensor Nodes

After the Intersection Criterion is met, any choice of two nodes results in small uncertainty of the target as shown in Figure 4.5c. A linear approximation of the shaded area can be represented as a parallelogram. By Theorem 3.1, the two nodes are selected if $sin^2\ \alpha$ is minimized, where the angle α is formed by the two nodes and the target.

4.4.3 Choice of Three Sensor Nodes

By Theorem 3.2, the third sensor node S_3 is selected given the first two S_1 and S_2. As shown in Figure 4.6, the S_3T is the bisector of the angle $\widehat{S_1TS_2}$.

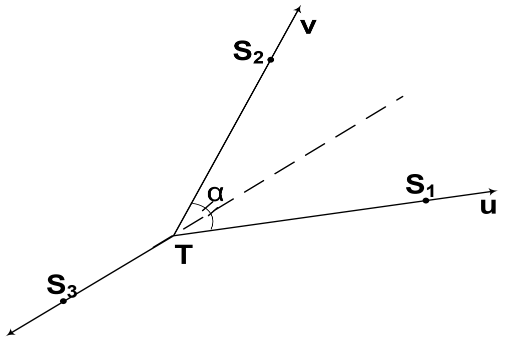

Figure 4.6: Choice of the third sensor

4.4.4 Choice of Four and More Sensor Nodes

According to Equation (4.5), the measurement covariance matrix Θ_k is given by

$$\Theta_k = E\{y_k y_k^T\} = (A_k^T A_k)^{-1} A_k^T \Phi_k A_k [(A_k^T A_k)^{-1}]^T \tag{4.13}$$

where $\Phi_k = E\{r_k r_k^T\}$.

By Theorem 3.5, the trilateration uncertainty $Trace(\Theta_k)$ is uniformly bounded. The fourth sensor is chosen so that $Trace(\Theta_k)$ is minimized.

4.5 Discussion

The covariance matrix Θ_k in (4.13) depends only on both: the angle α (formed between the two sensors and the target shown in Figure 4.6) and the measurement variance of each sensor. Two sensors S_1 and S_2, (whose angle between them and the target $\widehat{S_1 T S_2} = \alpha$) result in minimum trilateration error when $\alpha = 90°$. According to Theorem 3.2, the third sensor that minimizes trilateration errors is the sensor S_3 such that $S_3 T$ is the bisection of the angle $\widehat{S_1 T S_2}$ as shown in Figure 4.6.

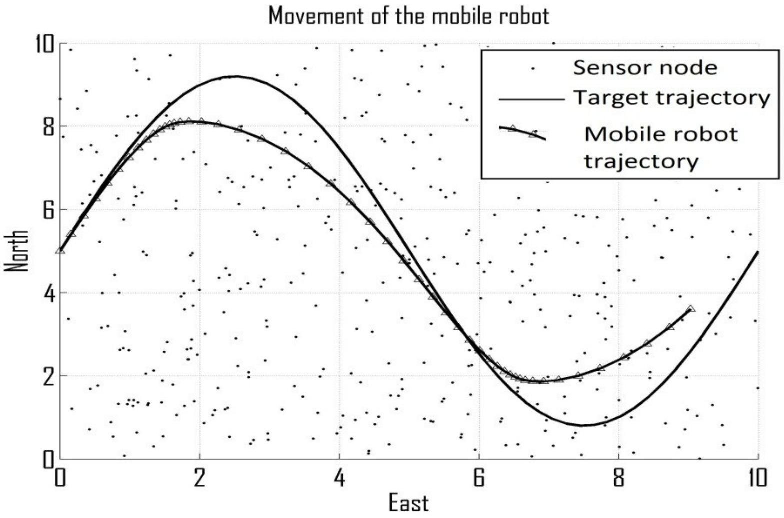

Figure 4.7: Movement of the mobile robot along a sinusoid trajectory

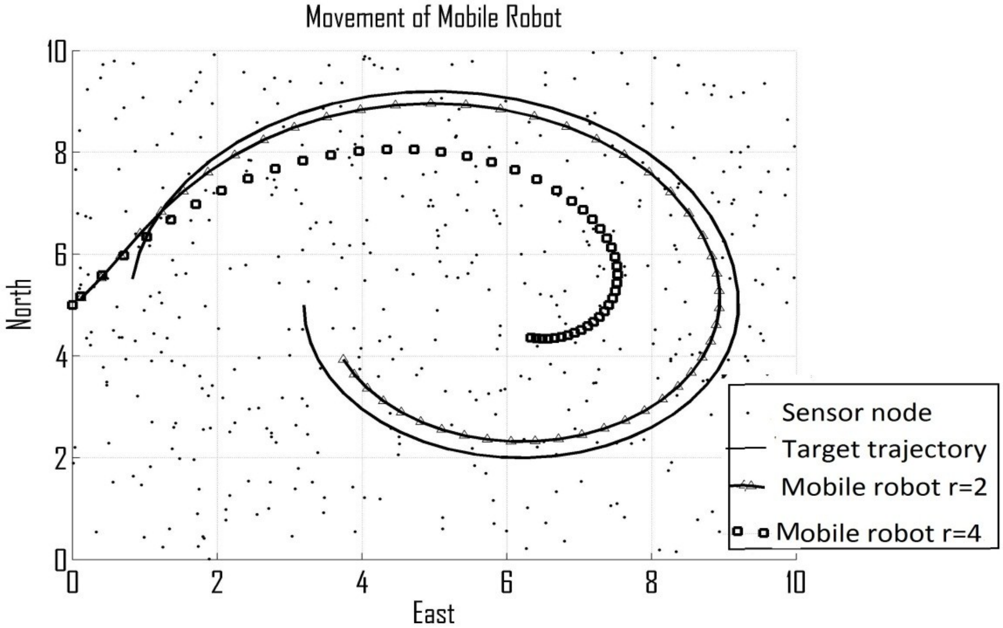

Figure 4.8: Movement of the mobile robot with different communication ranges. The dots, triangular and square symbols represent the trajectory of the target; trajectory of the mobile robot with communication range of 2.0; communication range of 4.0, respectively.

4.6 Numerical Examples

We considered some scenarios to demonstrate the effectiveness of the proposed system. The examples in this section refer to figures 4.7 - 4.10. Along the same lines as in chapter 3, the sensor field is assumed to be a square of the dimension 10×10 units, in which 441 sensor nodes are randomly deployed.

In Figure 4.7, the dots represent the locations of sensor nodes. The bold curve represents the trajectory of the target, while the curve with triangular symbol represents the trajectory of the mobile robot when the communication range was 2.5. When the target moves along a sinusoid trajectory, the mobile robot is expected to move in a similar fashion. However, as the target changes its heading, the mobile robot tends to be moving less and sometimes does not move at all.

4.7 Conclusion

In this chapter, we studied the use of a mobile robot working in conjunction with the WSN to track a target. A path is selected for the mobile robot such that the target is tracked while minimizing the total distance traveled by the robot. The proposed algorithm enables the selection of a minimum number of sensor nodes to track a target resulting in lower power consumption in the WSN. The overall tracking performance is enhanced through the implementation of a Kalman filter. It was shown that the proposed technique eliminates: the handover process between master nodes and the communication between the nodes and the network sink. Hence, the mobile robot can track the target more efficiently and reliably.

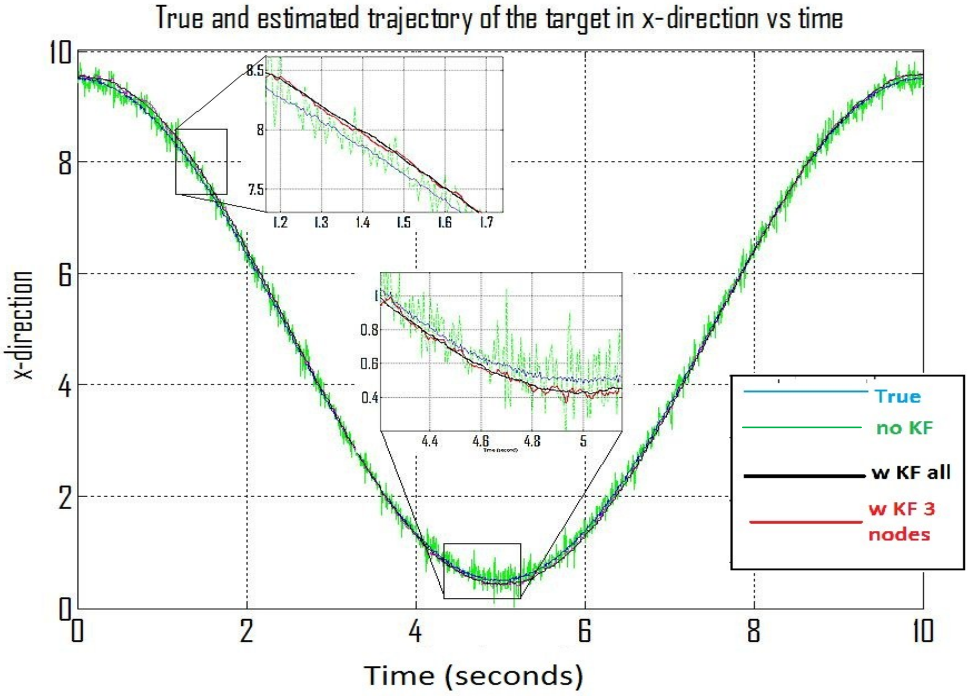

Figure 4.9: True and estimated trajectory of the target in one direction. Without using the Kalman filter, the tracking error was high and fluctuated as shown in green line. When the Kalman filters were used (black and red lines), the tracking errors were reduced.

Chapter 5

Enhancing the Life Time of a Wireless Sensor Network in Target Tracking Applications

In this chapter, we propose a method to enhance the life span of the WSN under the constraint of tracking quality. The problem is cast as an optimization problem to minimize the power consumption cost function under the constraint of tracking quality. The cost function accounts for both the residual power of each sensor node and its sensing task. The cost function increases when the residual power of a sensor node decreases or a sensing task requires more power. The improvement in the tracking performance obtained by the proposed method is demonstrated through numerical examples.

5.1 Introduction

Target tracking is one of the important applications of a Wireless Sensor Network (WSN). Difficulties in the deployment of WSNs and the limited capabilities of each node restrict their long term utility for most applications. Some of the challenges that need to be addressed are the energy consumption, useful life, and quality of information obtained using these networks. These problems take on added importance in target tracking applications where the target is dynamic and the sensor measurements are noisy.

Energy consumption and tracking quality [98] are two main challenges in tracking of a dynamic target using WSNs. To save energy consumption, Fang and Li [99] proposed a distributed estimation method for reducing communication and compressing data.

Other approach [100] minimized quantization error and transmission power. Lin at et. [101] investigated the energy-efficient multiple sensor scheduling, and calculated the optimal sampling time to meet the tracking performance. Several sensor activation schemes were used in [102] to reduce power consumption under the effect of tracking quality. Smart scheduling methods [87, 103] were proposed to activate appropriate sensors for the tracking and to deactivate the "low-quality" sensors. The main purpose of these methods is to save the energy consumption and to prolong the network life time. Moreover, the tracking quality metrics, defined in these works, did not address the relationship between trilateration uncertainty and geometric distribution of sensor nodes.

To track a dynamic target using range-measurement sensors, the trilateration uncertainty [51-55] is used as a main metric for tracking quality, which depends on both the sensors' locations and the location of the target as discussed in Chapter 3. Thus, a small number of sensor nodes can result in small tracking errors while a large number of nodes can result in poor tracking performance.

In this chapter, a method to improve the life span of the WSN while maintaining the desired level of tracking quality is proposed. The problem is formulated as an optimization problem where the power consumption is minimized under the constraint of tracking quality. The power consumption cost function depends on two parameters: the current residual power and the power expected to be consumed for a sensing mode. The cost is inversely proportional to the residual power of the node. Each sensor node operates in four modes (sleeping, active, sensing, and master mode) sorted as increasing power consumption; a sleeping node consumes much less power than a master node does. By minimizing the cost function under the constraint of trilateration uncertainty, the nodes with more residual power are scheduled for more power-intensive tasks, while the nodes with low battery power are scheduled to be in sleeping mode. The selection algorithm is suboptimal while the computational cost is significantly reduced. Another aspect of the algorithm is that it is implemented in a distributed manner, and is scalable to a network of a larger number of sensor nodes. The Kalman filter is proposed to further improve tracking quality. At a time instant, only one master node plays a role as the fusion center, which runs the Kalman filter and the selection algorithm.

5.2 Problem Formulation

We consider the problem of target tracking using a wireless sensor network. A two-dimensional sensor field is densely deployed with stationary sensor nodes, which are equipped with transceivers, computational platforms, and range measurement units. When a target is in the sensing field, the challenge is the scheduling of sensor nodes: which sensors should be in sleeping mode; which sensors sense the target; which sensors run the tracking algorithm. Due to the effect of geometric dilution of precision, the spatial distribution of selected sensor nodes affects the performance of the trilateration algorithm. In order to extend the life time of a sensor network, sensors with more residual power are preferable to low residual power ones. The proposed power consumption cost for using a specific sensor is a deceasing function with respect to its residual power. The optimization problem is to choose a set of sensor nodes that minimize the power cost function while still meeting the constraint of trilateration uncertainty. The sensor selection algorithm also enables the distributed implementation of the tracking algorithm, i.e., Kalman filter.

5.2.1 Power Consumption Model and Cost Function

The power consumption cost function accounts for two conditions: the residual power of each node and its operating modes. To simplify the problems, it is assumed that each node has four operating modes (sorted as increasing power consumption) including: sleeping mode, active mode, sensing mode, and master mode. Moreover, the power consumption of each sensor in a particular operating mode is constant.

Let N be the number of sensor nodes in the sensor field. Let $s = [s_1, s_2, \dots s_N]^T$, where s_i represents the operating mode of the ith node, and $s_i \in \{0, 1, 2, 3\}$ (the values $0, 1, 2$ and 3 represent sleeping, active, sensing, and master mode, respectively).

Let the residual power of a node be x (if $x = 0$, the node is depleted, while $x = c$ the node has its full power). Let $p: [0, c] \mapsto (0, \infty)$ be a continuous and decreasing function. Let the operating mode of the i^{th} node be s_i, and let $\mathscr{s}_i$ be the total amount of power consumed in a tracking interval. The power consumption cost for the i^{th} node is defined as

$$c_i = \int_x^{x+\mathscr{s}_i} p(t)dt. \tag{5. 1}$$

The total cost function of the network is $\boldsymbol{c}_{total} = \sum_{i=1}^{N} c_i$.

5.2.2 Power Saving Optimization Problem

Let $\mathcal{P}$ be the power set of all the possible combination of of all the nodes' operating mode. The size of $\mathcal{P}$ is 4^N.

Let $\mathscr{t}: \mathcal{P} \mapsto \mathbb{R}$ be a trilateration quality set function such that

$$\mathscr{t}(s) = Trace(\Theta_k). \tag{5. 2}$$

Where Θ_k is the trilateration uncertainty computed by (8) with the sensor nodes with $s_i = 2$.

Let $\mathscr{p}: \mathcal{P} \mapsto \mathbb{R}$ be the power consumption cost function such that

$$\mathscr{p}(s) = \sum_{i}^{N} \int_{p_i}^{p_i + \mathscr{s}_i} p(t)dt \tag{5. 3}$$

where p_i, s_i, and $\mathscr{s}_i$ are the residual power, operating mode, and power consumption, respectively, in one tracking interval of the ith node.

Given a predefined bound on uncertainty error B our optimization problem is:

$$\begin{gathered} \text{minimize}\, \mathscr{p}(s) \\ \text{subject to}\, \mathscr{t}(s) < B \end{gathered} \tag{5. 4}$$

To solve this problem we divide it into three small problems: selection of the master node, selection of sensing nodes, and finally selection of the active nodes.

5.3 Algorithm and Analysis

In this section, the algorithm for selecting the master node, sensing nodes, and active nodes are discussed. Since only sensing nodes affect the performance of the trilateration algorithm (i.e., matrix Θ_k), the master node, sensing nodes, and active nodes can be selected independently in terms of trilateration quality function $t(s)$ in (5.4).

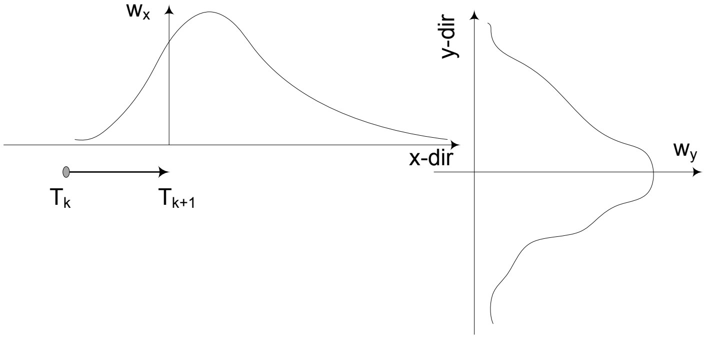

Figure 5.1: Distribution functions of the master node. The distribution of the cost function in the heading of the target should be the heavy tailed, and distributed of the cost function in the y-direction should be bell shape.

5.3.1 Selection of Master Nodes

During each tracking interval, the master node transmits a broadcast message, receives data messages from the nodes within the measurement range of the target, and computes the Kalman filter. The master node consumes more power than other nodes; hence, the node with more residual power is preferred. On the other hand, the master node should be in the heading direction of the target so that the hand-over process can be kept less frequent. The choice of the master node does not affect the choice of the sensing nodes in terms of tracking performance, but it has an effect on the total power consumption cost function.

Suppose that the current location of the target at time k is T_k and the estimated position of the target at time $k + 1$ is T_{k+1}. The heading direction of the target $\overrightarrow{T_k T_{k+1}}$ is coincident with the x-direction. The optimal distribution function of the master node should be

$$w_{master} = w_x w_y. \qquad (5.5)$$

Where w_x and w_y, the bell shapes as shown in Figure 5.1, are distribution of the master node in x and y directions respectively. The optimal position of the master node is the position that w_{master} is maximized.

Let ρ_x be the total normalized power consumption cost a master node and the cost for transmitting data packet to the network sink. The weighted cost function for selection the sensor node is

$$W = \alpha\rho_x + \beta w_{master}. \qquad (5.6)$$

Where α, and β are weight constants, and $\alpha + \beta = 1$.

5.3.2 Selection of Active Sensor Nodes

The active nodes that are in the sensing radius and along the heading of the target are selected based on the method proposed in Chapter 2.

5.3.3 Schedule and Selection Algorithm

After the master node and the active nodes are selected, the following algorithm will choose the set of sensing nodes that minimize the power consumption cost function.

The inputs of the algorithm are: n_k sensor nodes $\mathcal{S}_n = \left[S_1, S_2, \dots, S_{n_k}\right]$, the target coordinate T, their residual power p_i for $i = 1 \div n_k$, and range measurement d_i for $i = 1{:}\, n_k$. The output is a set of selected sensors $[S^1, S^2, S^3] \subseteq \mathcal{S}_n$.

The main idea of the algorithm is the use of heuristic ranking system which depends on the power consumption cost. The suboptimal approach is to minimize the total indices of the sorted costs. Instead of minimizing the total cost $\boldsymbol{c}_{total} = \sum_{i=1}^{3} c_i$, the algorithm minimizes their sum of indices $i + j + k$.

Step 1: Calculate the power costs $c_i = \int_{p_i}^{p_i+\mathscr{s}_2} p(t)dt$ ($\mathscr{s}_2$ represents the sensing task) for each sensor by equation (5.1), and sort the cost such that

$$c_1 \leq c_2 \leq \ \dots \ \leq \ c_{n_k}.$$

Step 2: Eliminate collinear nodes. If two or more sensor nodes together with the target are collinear or closed to collinear, all the nodes are eliminated from the selection pool except 2 nodes with maximum residual power. After the collinear elimination processes, no set of three collinear sensor nodes exists. Thus, nodes with large trilateration uncertainty are eliminated.

Step 3. Search for three best nodes that minimized the power consumption cost.

For each set (i, j, k), $1 \leq i, j, k \ \leq n_k$.

- **Calculate** $\mathscr{t}(s)$ by (5.2) for nodes, $s = [S_i, S_j, S_k]$, if $\mathscr{t}(s) \leq B$ (B is predefined trilateration uncertainty).
- **Choose** (i, j, k) such that $\mathscr{p}(s)$ in (5.3) is maximized.

Theorem 5.1: The algorithm above results in the suboptimal solution of the optimization problem (5.4).

Proof: Suppose that a solution of the algorithm is the set $s = [S_i, S_j, S_k]$, and $Sm = i + j + k$. Clearly,

$$c^0 = \min_{Sm=i+j+k} \mathscr{p}(s) = \min_{Sm=i+j+k} \ c_{total} \tag{5. 7}$$

Let $s' = [S_{i\prime}, S_{j\prime}, S_{k\prime}]$ be another solution of the problem (5.4).

Obliviously, $i' + j' + k' \geq Sm$ due to the condition for the algorithm to stop. There exists a set $[i^o, j^o,\ k^0]$ such that

$$\begin{cases} i' \geq i^0 \\ j' \geq j^0 \\ k' \geq k^0 \\ i^o + j^o + k^0 = Sm \end{cases}$$

Hence, $c_{i'} \geq c_{i^0}$, $c_{j'} \geq c_{j^0}$, and $c_{k'} \geq c_{k^0}$ and by (2.7)

$$\wp(s') = \wp([S_{i'}, S_{j'}, S_{k'}]) \geq \wp([S_{i^0}, S_{j^0}, S_{k^0}]) \geq \wp(s) = c^0.$$

Thus, s is the optimal solution for the Step 3. Since some sensor nodes are eliminated by Step 2, the solution is suboptimal.

5.4 Discussion

5.4.1 Selection of the Power Cost Function

In equation (5.1), power profile function $p(t)$ is a decreasing continuous function and it is selected based on the characteristic of a specific type of sensor nodes and on the power management strategy.

5.4.2 Selection of the Master Node

In equation (5.6), if α is large, the weighted cost depends more on the current residual power of the sensor and its cost to transmit data to the network sink. If $\alpha = 1$, (or $\beta = 0$) the node with lowest power consumption cost is selected, but it can be outside the communication range of the target's sensed nodes in the next tracking interval. On the other hand, if $\alpha = 0$ (or $\beta = 1$), the selected master node is in the heading of the target, but its residual power may be low.

5.4.3 The Selection Algorithm

In worst case scenario, the calculation time of the selection algorithm is equal to that of exhaustive search. However, the proposed algorithm performs much better in practice.

5.5 Numerical Example

The following example uses a sensor field of dimensions 10×10 units to demonstrate the selection of a minimum number of sensor nodes and implementation of distributed Kalman filter for target tracking. Assume that 441 sensor nodes are randomly deployed in this sensor field. The power consumption profile using in the simulation was based on the analysis in [1], even though our approach did not depend on any specific hardware platform. Let P_{Tx}, P_{Rx}, P_{Active}, P_{Sens}, P_{Sleep}, and P_{Comp} be the transmitting power, receiving power, active power, sensing power, sleeping power, and computational power respectively. The power consumption in each operation modes is defined as follows.

- Sleeping mode: $\mathscr{s}_0 = P_{Sleep}$.
- Active mode: $\mathscr{s}_1 = P_{Rx} + P_{Active}$.
- Sensing mode: $\mathscr{s}_2 = P_{Rx} + P_{Sens} + P_{Tx} + P_{Active}$.
- Master mode $\mathscr{s}_3 = P_{Tx} + nP_{Rx} + P_{Comp} + P_{Active}$ where n is the number of sensing nodes.

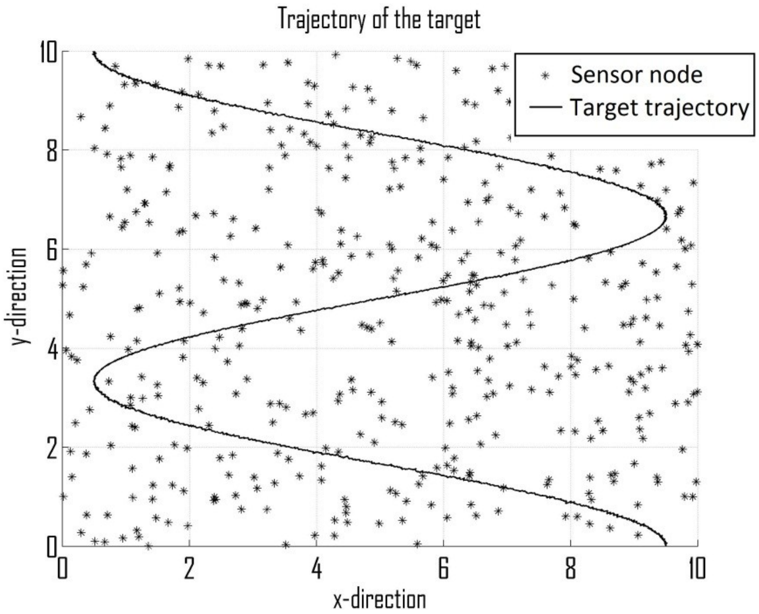

Figure 5.2: Trajectory of the target and distribution of the sensor nodes.

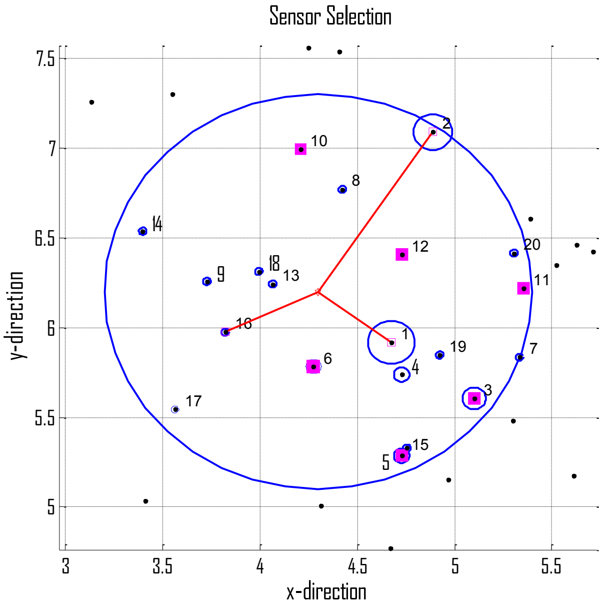

Figure 5.3: The sensor nodes represent by the dots. Radiuses of small circles are proportional to the residual power of sensor nodes. The squares represent the small group of sensors left after running the collinear elimination algorithm. The sensors inside the big circle are able to sense the target. Three sensors #1, #2, and #16 minimized the power cost while still satisfying the required trilateration uncertainty. Meanwhile, three sensors #1, #2, #3 yielded the minimum power consumption cost, but did not meet the trilateration uncertainty condition.

The target was assumed to move along a sinusoid trajectory as shown in Figure 5.2. The sensing radius was 1.4, and the simulation time was 10 seconds. The measurement noise variance σ_V=0.1, and the state noise variance $\sigma_S = 0.005$.

In Figure 5.3, the target were at (4.3, 6.2), and the sensing radius was 2.0. 20 nodes within the sensing range of the target were assumed to have uniformly random residual power. The trilateration constraint was $B = 5\sigma_V$ in equation (5.4).

The overall tracking performance along the x-direction is shown in Figure 5.4. The tracking performance was improved by using the Kalman filter. The true coordinate of the target was 9.5 in x-direction while the initial value for the filter was 8.0. The estimated error was initially high, but it reduced greatly after about 0.3 second. The tracking performance (in black solid line) of three nodes (which resulted in minimum trilateration uncertainty) was better the performance of three nodes (red line) – which resulted in minimum power consumption cost. However, as shown in the Figure 5.4, the difference was not significant.

In Figure 5.5, the average number of sensed nodes before collinear elimination was 24.3, which resulted in 2,529 exhaustive search attempts. After collinear elimination, only average 6.1 sensed nodes remained, which the average total search attempts reduced to 27.9 while the average actual search attempts were 19.5.

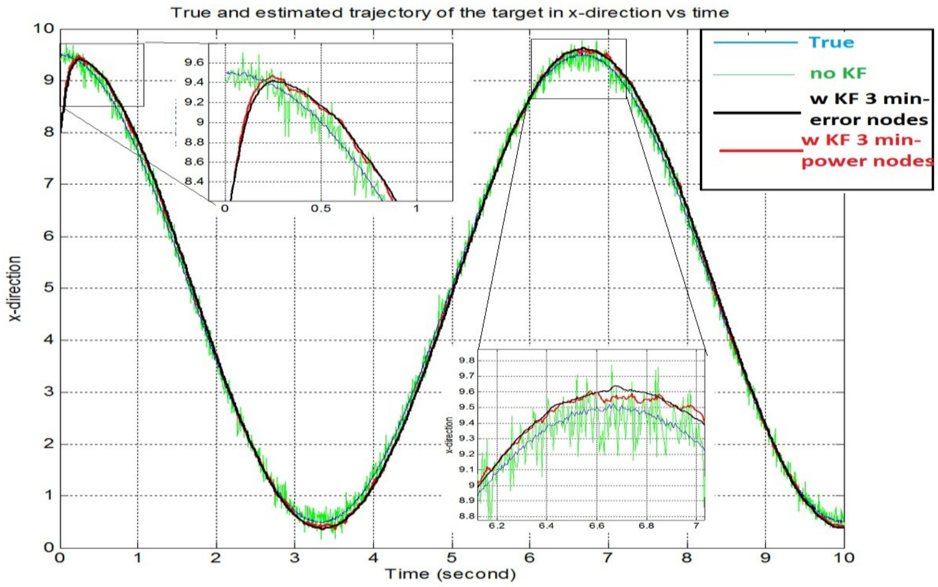

Figure 5.4: True and estimated trajectory of the target in x-direction. Without using the Kalman filter, the tracking error was high and fluctuated as shown in green line. When the Kalman filters were used (black and red line), the tracking errors were reduced. The red line was the performance when three nodes (which minimized power cost) were used. When three nodes (which minimized trilateration uncertainty) were used for tracking (black line), the tracking error is smaller and smother

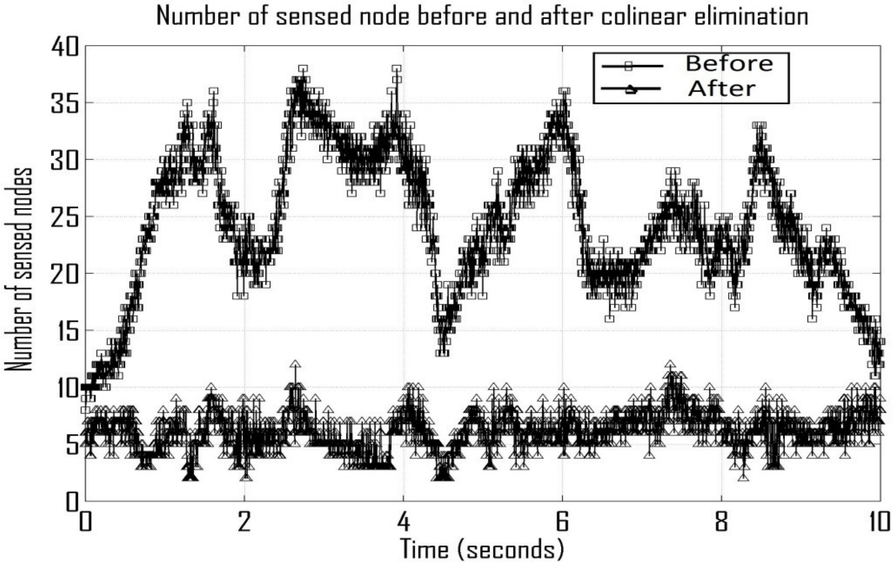

Figure 5.5: Number of sensed nodes before and after collinear elimination

5.6 Conclusion

In this chapter, a solution for the optimization problem to minimize the power cost function of a WSN was proposed. The algorithm reduced the computational complexity and extended the life time of the network while satisfying the required tracking quality. Nodes with more residual power were preferred for power intensive tasks while nodes with low residual power were scheduled to sleep. The numerical examples show that the validity of the proposed approach.

Chapter 6

Conclusions and Scope for Future Work

The tracking of a single target using a WSN was investigated in this dissertation. The sensor nodes were assumed to be stationary, have sensing and communication capabilities, and densely deployed in the region of interest. Further, the sensed information is transmitted to a network sink in a multi-hop fashion or through a cluster head that is one hop from the sensor node. The tracking of target using range-only sensors was divided into four small problems: implementing the distributed Kalman filter to reduce tracking error; analyzing the uncertainty of trilateration algorithm and tracking the target with minimum number of sensor nodes; using a mobile robot to assist the tracking for improving reliability and performance; and increasing the life span of the network.

The background of WSNs including issues such as deployment and coverage, MAC protocols, Routing protocols, and their applications were covered in Chapter 1. Consequently, the target tracking problem using a WSNs was surveyed. To track a dynamic target, the WSN has to localize the target first by localization methods (e.g., trilateration or triangulation), and then applying estimation techniques (e.g., Kalman filters or particle filters) to enhance the tracking performance. The use of autonomous vehicles and the energy efficiency issues were also reviewed.

In Chapter 2, distributed Kalman filter was implemented in a WSN to track dynamic targets. The approach was distributed in the sense that, at an instant, only one master node executes the Kalman filter using the range estimates from a set of sensor nodes in the proximity of the target. Several factors affecting the tracking quality are studied including velocity of the target, variance of the measurement noise, nonlinear trajectory of the target, number of sensor nodes used for tracking, and the retention of learned knowledge (i.e., states of the target and covariance matrix). The total power consumption was shown to decrease as the number of sensors (used for tracking) decreased. However, the trade-off was that the tracking quality also decreased. Mathematical proofs were developed to study the convergence of the estimated errors. Numerical simulations showed that the quality of tracking improved significantly with the use of Kalman filter.

The uncertainty in the localization of the target through trilateration was rigorously analyzed in Chapter 3. The analysis showed that a small set of nodes is adequate to guarantee small trilateration errors. Increasing the number of nodes used for trilateration could result in large localizing errors. By understanding the relationship between trilateration uncertainty and the spatial distribution of sensor nodes, an algorithm was developed that could choose a set of minimum number of sensor nodes to effectively track the target.

In Chapter 4, the use of a mobile robot in conjunction with the WNS was proposed to track target more efficiently and reliably. The mobile robot, equipped with powerful computational platform, eliminated both the hand-over process among sensor nodes and the need to transmit data from the sensors to the network sink. This significantly reduced the power consumption of WSNs and improved the tracking quality. The moving strategy of the mobile robot assured that its traversed path was minimized and within one-hop communication of the sensor nodes (which measured the distances to the target).

The central topic of Chapter 5 was to enhance the life time of the WSN. The problem was cast as an optimization problem that minimized the power consumption cost under the constraint of tracking quality (i.e., trilateration uncertainty). The cost function accounted for both the residual power and the computational requirement of each sensor node. The cost is inversely proportional to the residual power and directly proportional to the computational overhead of a node. The trilateration uncertainty was chosen as a quality metric. The optimization problem was solved by heuristic ranking method and linear elimination process. Numerical analysis showed that the algorithm was computationally efficient, and more importantly, extended the life span of the WSN.

The dissertation opens some questions for future research. One of the questions that has to be addressed is the procedure for the tracking systems to deal with issues such as error in synchronization of the clocks on the sensor nodes, error in locations of sensor nodes, and the dependence of measurement noise on the distance to the target.

In this dissertation, the mobile robot was assumed to be able to move independently in the sensor field. In reality, however, the mobility of the robot can be limited by obstacles. The robot might also not have a direct line to sight to the network sink causing it to the sink through multiple communication hops. The path planning in such circumstances is bound to affect the tracking performance of the system. The practical deployment of mobile robots to augment WSN in tracking multiple dynamic targets is another area that future research has to address.

References

[1] M. K. Watfa and S. Commuri, "Optimal sensor placement for Border Perambulation," in *2006 IEEE International Conference on Control Applications*, Munich, Germany, 2006.

[2] G. Wang, G. Cao, and T. F. L. Porta, "Movement-Assisted Sensor Deployment," *IEEE Transaction on Mobile Computing,* vol. 5, pp. 640-652, 2006.

[3] S. Poduri, S. Pattem, B. Krishnamachari, and G. S. Sukhatme, "Using Local Geometry for Tunable Topology Control in Sensor Networks," *IEEE Transaction on Mobile Computing,* vol. 8, pp. 218-230, 2009.

[4] X.-Y. Li, P.-J. Wan, and O. Frieder, "Coverage in Wireless Ad Hoc Sensor Networks," *IEEE Transaction on Computers,* vol. 52, pp. 753-763, 2003.

[5] W. Wang, V. Srinivasan, B. Wang, and K.-C. Chua, "Coverage for Target Localization in Wireless Sensor Networks," *IEEE Transaction on Wireless Communications,* vol. 7, pp. 667-676, 2008.

[6] H. M. Ammari and S. K. Das, "A Study of k-Coverage and Measures of Connectivity in 3D Wireless Sensor Networks," *IEEE Transaction on Computers,* vol. 59, pp. 243-257, 2010.

[7] M. K. Watfa and S. Commuri, "The 3-Dimensional Wireless Sensor Network Coverage Problem," in *2006 IEEE International Conference on Networking, Sensing and Control. ICNSC '06*, Ft. Lauderdale, FL, pp. 856-861, 2006.

[8] J. Polastre, J. Hill, and D. Culler, "Versatile low power media access for wireless sensor networks," in *SenSys '04 Proceedings of the 2nd international conference on embedded networked sensor systems*, New York, NY, USA, 2004.

[9] I. Demirkol, C. Ersoy, and F. Alagöz, "MAC protocols for wireless sensor networks: a survey " *IEEE Communications Magazine,* vol. 44, pp. 115-121, May 2006.

[10] J. N. Al-Karaki and A. E. Kamal, "Routing techniques in wireless sensor networks: a survey," *Wireless Communications, IEEE,* vol. 11, pp. 6-28, 2004.

[11] I. F. Akyildiz, W. Su, Y. Sankarasubramaniam, and E. Cayirci, "A survey on sensor network," *IEEE Communications Magazine,* vol. 40 pp. 102-114, August 2002.

[12] C.-Y. Chong and S. P. Kumar, "Sensor networks: evolution, opportunities, and challenges," in *Proceedings of the IEEE* pp. 1247 - 1256, 2003.

[13] X. Chang, R. Tan, G. Xing, Z. Yuan, C. Lu, Y. Chen, and Y. Ya, "Sensor Placement Algorithms for Fusion-Based Surveillance Networks," *IEEE Transaction on Parallel and Distributed Systems,* vol. 22, 2011.

[14] Y. Yang and R. S. Blum, "Sensor Placement in Gaussian Random Field Via Discrete Simulation Optimization," *IEEE Signal Processing Letters,* vol. 15, pp. 729-732, 2008.

[15] X. Bai, C. Zhang, D. Xuan, and W. Jia, "Full-Coverage and k-Connectivity (k=14,6) Three Dimensional Networks," in *The 28th Conference on Computer Communications (INFOCOM)*, Rio de Janeiro, Brazil, pp. 388 - 396, 2009.

[16] Z. Cheng, M. Perillo, and W. B. Heinzelman, "General Network Lifetime and Cost Models for Evaluating Sensor Network Deployment Strategies," *IEEE Transaction on Mobile Computing,* vol. 7, pp. 484-497, 2008.

[17] Y. Wang and P. Ishwar, "Distributed Field Estimation With Randomly Deployed, Noisy, Binary Sensors," *IEEE Transaction on Signal Processing,* vol. 57, 2009.

[18] S. Meguerdichian, F. Koushanfar, M. Potkonjak, and M. B. Srivastava, "Coverage Problems in Wireless Ad-hoc Sensor Networks," in *IEEE INFOCOM 2001 - The Conference on Computer Communications* Alaska, USA, 2001.

[19] M. Cardei, M. T. Thai, Y. Li, and W. Wu, "Energy-efficient target coverage in wireless sensor networks," in *INFOCOM 2005. 24th Annual Joint Conference of the IEEE Computer and Communications Societies*, Miami, Florida, 2005.

[20] C. S. R. Murthy and B. S. Manoj, *Ad Hoc Wireless Networks Architectures and Protocols*: Prentice Hall, 2004.

[21] V. Rajendran, K. Obraczka, and J. J. GarciaLunaAceves, "Energy Efficient, Collision Free Medium Access Control for Wireless Sensor Networks," in *Proceedings of the 1st international conference on embedded networked sensor systems*, 2003.

[22] V. Kanodia and C. Li, "Distributed Priority Scheduling and Medium Access in Ad-hoc Networks," *ACM Journal Wireless Networks,* vol. 8, 2002.

[23] W. Ye, J. Heidemann, and D. Estrin, "Medium Access Control with Coordinated Adaptive Sleeping for Wireless Sensor Networks," *IEEE/ACM Transactions on Networking,* vol. 12, pp. 493-506, 2004.

[24] P. Lin, C. Qiao, and X. Wang, "Medium Access Control with a Dynamic Duty Cycle for Sensor Networks," in *2004 IEEE Wireless Communications and Networking Conference*, pp. 1534 - 1539, 2004.

[25] G. Lu, B. Krishnamachari, and C. S. Raghavendra, "Adaptive Energy-Efficient and Low-Latency MAC for Data Gathering in Wireless Sensor Networks," in *Proceedings of the 18th International Parallel and Distributed Processing Symposium (IPDPS'04)*, 2004.

[26] Y. C. Tay, K. Jamieson, and H. Balakrishnan, "Collision-Minimizing CSMA and Its Applications to Wireless Sensor Networks," *IEEE Journal of Selected Areas in Communication,* vol. 22, pp. 1048 - 1057, 2004.

[27] T. Zheng, S. Radhakrishnan, and V. Sarangan, "PMAC: An Adaptive Energy-Efficient MAC Protocol for Wireless Sensor Networks," in *Proceedings of the 19th IEEE International Parallel and Distributed Processing Symposium (IPDPS'05)*, Denver, Colorado, pp. 65-72, 2005.

[28] J. N. Al-Karaki and A. E. Kamal, "Routing techniques in wireless sensor networks: a survey " *IEEE Wireless Communications Magazine,* vol. 11, pp. 6-28, 2004.

[29] J. Kulik, W. Heinzelman, and H. Balakrishnan, "Negotiation-based protocols for disseminating information in wireless sensor networks," *ACM Journal Wireless Networks,* vol. 8, pp. 169-185, March-May 2002.

[30] K. Sohrabi and J. Pottie, "Protocols for self-organization of a wireless sensor network," *IEEE Personal Communications,* vol. 7, pp. 16-27, 2000.

[31] C. Intanagonwiwat, R. Govindan, and D. Estrin, "Directed Diffusion: A Scalable and Robust Communication Paradigm for Sensor Networks," in *In Proceedings of the Sixth Annual International Conference on Mobile Computing and Networking*, 2000.

[32] W. Heinzelman, A. Chandrakasan, and H. Balakrishnan, "Energy-Effcient Communication Protocol for Wireless Microsensor Networks," in *Proceedings of the 33rd Hawaii International Conference on System Sciences (HICSS '00)*, Hawaii, USA, 2000.

[33] S. Lindsey and C. Raghavendra, "PEGASIS: Power-efficient gathering in sensor information systems " in *IEEE Aerospace Conference Proceedings*, pp. 1125-1130, 2002.

[34] Y. Xu, J. Heidemann, and D. Estrin, "Geography-informed Energy Conservation for Ad-hoc Routing," in *Proceedings of the Seventh Annual ACM/IEEE International Conference on Mobile Computing and Networking*, Rome, Italy, 2001.

[35] Y. Yu, D. Estrin, and R. Govindan, "Geographical and Energy-Aware Routing: A Recursive Data Dissemination Protocol for Wireless Sensor Networks," UCLA Computer Science Department Technical ReportMay 2001.

[36] Y. Xiao, K. Thulasiraman, and G. Xue, "QoS Routing in Communication Networks: Approximation Algorithms Based on the Primal Simplex Method of Linear Programming," *IEEE Transaction on Computers,* vol. 55, pp. 815-829, 2006.

[37] L. Chen and W. B. Heinzelman, "QoS-Aware Routing Based on Bandwidth Estimation for Mobile Ad Hoc Networks," *IEEE Journal on Selected Areas in Communications,* vol. 23, pp. 561-572, March 2005.

[38] C. E. Perkins and P. Bhagwat, "Highly dynamic Destination-Sequenced Distance-Vector routing (DSDV) for mobile computers," in *ACM SIGCOMM '94 conference on Communications architectures, protocols and applications* 1994.

[39] J. J. Garcia-Luna-Aceves and M. Spohn, "Source-tree routing in wireless networks," in *IEEE Seventh International Conference on Network Protocols (ICNP '99)* pp. 273 - 282, 1999.

[40] C. E. Perkins and E. M. Royer, "Adhoc OnDemand Distance Vector Routing," 1999.

[41] R. Sivakumar, P. Sinha, and V. Bharghavan, "CEDAR: A Core-Extraction Distributed Ad Hoc Routing Algorithm," *IEEE Journal on Selected Areas in Communications,* vol. 17, pp. 1454-1465, 1999.

[42] Z. J. Haas, "A new routing protocol for the reconfigurable wireless networks," in *IEEE 6th International Conference on Universal Personal Communications Record*, San Diego, CA , USA, 1997.

[43] P. Bonato, "Clinical applications of wearable technology," in *Annual International Conference of the IEEE on Engineering in Medicine and Biology Society*, Minneapolis, Minnesota, 2009.

[44] Krishna Chintalapudi, T. Fu, J. Paek, N. Kothari, S. Rangwala, J. Caffrey, R. Govindan, E. Johnson, and S. Masri, "Monitoring civil structures with a wireless sensor network " *IEEE Internet Computing,* vol. 10, pp. 26 - 34, 2006.

[45] S. Kumar and D. Shepherd, "SensIT: Sensor Information Technology For the Warfighter," in *4th International Conference on Information Fusion*, Montréal, Québec, Canada, 2001.

[46] C. Alippi, R. Camplani, C. Galperti, and M. Roveri, "A Robust, Adaptive, Solar-Powered WSN Framework for Aquatic Environmental Monitoring," *IEEE Sensors Journal,* vol. 11, pp. 45 - 55 2011.

[47] M. Chen, S. Gonzalez, and V. C. M. Leung, "Applications and design issues for mobile agents in wireless sensor networks," *IEEE Wireless Communications,* vol. 14, pp. 20-26, December 2007.

[48] J. O'Rourke, *Computational Geometry in C*, Cambridge University Press, 1998.

[49] D. Munoz, F. Bouchereau, C. Vargas, and R. Enriquez-Caldera, *Position Localation Techniques and Applications*, 2009.

[50] http://www.gps.gov/

[51] B. T. Fang, "Trilateration and Extension to Global Positioning System Navigation," *Journal of Guidance, Control, and Dynamics,* vol. 9, pp. 715-717, 1986.

[52] D. E. Manolakis, "Efficient solution and performance analysis of 3-D position estimation by trilateration," *IEEE Transaction on Aerospace and Electronic Systems,* vol. 32, pp. 1239-1248, 1996.

[53] J. W. Powers, "Range Trilateration Error Analysis," *IEEE Transaction on Aerospace and Electronic Systems,* vol. AES-2, p. 572, July 1966.

[54] F. Thomas and L. Ros, "Revisiting trilateration for robot localization," *IEEE Transaction on Robotics,* vol. 21, pp. 93-101, February 2005.

[55] Z. Yang and Y. Liu, "Quality of Trilateration: Confidence-Based Iterative Localization," *IEEE Transaction on Parallel and Distributed Systems,* vol. 21, pp. 631-640, June 2008.

[56] H. L. Groginsky, "Position Estimation Using Only Multilple Simultaneous Range Measurements," *IRE Transaction on Aeronautical and Navigational Electronics,* vol. ANE-6, pp. 178-187, September 1959.

[57] R. J. Pieper, A. W. Cooper, and G. Pelegris, "Passive range estimation using dual baseline triangulation," *Optical Engineering,* vol. 35, 1996.

[58] S. Shams, "Neural network optimization for multi-target multi-sensor passive tracking," *IEEE Proceeding of the IEEE,* vol. 84, pp. 1442-1457, 1996.

[59] V. Isler, "Placement and distributed deployment of sensor teams for triangulation based localization," in *IEEE International Conference on Robotics and Automation*, Orlando, FL, pp. 3095-3100, 2006.

[60] R. Kalman, "A New Approach to Linear Filtering and Prediction Problems," *Transactions of the ASME--Journal of Basic Engineering,* vol. 82, pp. 35-45, 1960.

[61] T. Kailath, A. H. Sayed, and B. Hassibi, *Linear Estimation*, Prentice-Hall, Inc., 2000.

[62] Y. Song and J. W. Grizzle, "The Extended Kalman Filter as a Local Asymptotic Observer for Nonlinear Discrete-Time Systems," *Journal of Mathematical Systems, Estimation and Control,* vol. 5, pp. 59-78, 1995.

[63] K. Reif, S. Gunther, E. Yaz, and R. Unbehauen, "Stochastic stability of the discrete-time extended Kalman filter," *IEEE Transaction on Automatic Control,* vol. 44, pp. 714-728, 1999.

[64] R. Schutz, R. McAllister, B. Engelberg, V. Maone, R. Helm, V. Kats, C. Dennean, W. Soper, and L. Moran, "Combined Kalman filter (CKF) and JVC algorithms for AEW target tracking applications," in *Proceedings-SPIE the international society for optical engineering*, pp. 164-175, 1997.

[65] D. Bizup and D. Brown, "The over-extended Kalman filter - don't use it!," in *Proceedings of the Sixth International Conference of Information Fusion,* pp. 40-46, 2003.

[66] F. S. Cattivelli, C. G. Lopes, and A. H. Sayed, "Diffusion strategies for distributed Kalman filtering: formulation and performance analysis," in *Proc. 2008 IAPR Workshop on Cognitive Information Processing*, Santorini, Greece, 2008.

[67] H. R. Hashemipour, S. Roy, and A. J. Laub, "Decentralized structures for parallel Kalman filtering," *IEEE Transaction on Automatic Control,* vol. 33, pp. 88-94, 1998.

[68] J.-H. Kim, M. West, E. Scholte, and S. Narayanan, "Multiscale consensus for decentralized estimation and its application to building systems," in *2008 American Control Conference*, Seattle, WA pp. 888-893, 2008.

[69] G. O. Mutambara, *Decentralized estimation and control for multisensor systems*, CRC Press, 1998.

[70] R. Olfati-Saber, "Distributed Kalman filtering for sensor networks," in *46th IEEE Conference on Decision and Control*, New Orleans, LA pp. 5492 - 5498, 2007.

[71] R. Olfati-Saber and J. S. Shamma, "Consensus Filters for Sensor Networks and Distributed Sensor Fusion," in *44th IEEE Conference on Decision and Control, CDC-ECC'05*, pp. 6698 - 6703, 2005.

[72] B. S. Rao and H. F. Durrant-Whyte, "Fully decentralized algorithm for multisensor Kalman filtering," *IEE Proceedings-D Control Theory & Application,* vol. 138, pp. 413 - 420, September 1991.

[73] B. Ristic, S. Arulampalam, and N. Gordon, *Beyond the Kalman filter: Particle Filters for Tracking Applications*, Artech Print on Demand, 2004.

[74] M. S. Arulampalam, S. Maskell, N. Gordon, and T. Clapp, "A Tutorial on Particle Filters for Online Nonlinear/Non-Gaussian Bayesian Tracking," *IEEE Transaction on Signal Processing,* vol. 50, 2002.

[75] F. Gustafsson, F. Gunnarsson, N. Bergman, U. Forssell, J. Jansson, R. Karlsson, and P.-J. Nordlund, "Particle filters for positioning, navigation, and tracking," *IEEE Transaction on Signal Processing,* vol. 50, pp. 425-436, 2002.

[76] O. Ozdemir, R. Niu, and P. K. Varshney, "Tracking in Wireless Sensor Networks Using Particle Filtering: Physical Layer Considerations," *IEEE Transaction on Signal Processing,* vol. 57, pp. 1987-1999, 2009.

[77] J. Vermaak, S. J. Godsill, and P. Perez, "Monte Carlo filtering for multi target tracking and data association," *IEEE Transaction on Aerospace and Electronic Systems,* vol. 41, pp. 309-332, 2005.

[78] P. Benavidez and M. Jamshidi, "Mobile Robot Navigation and Target Tracking System," in *6th International Conference on System of Systems Engineering*, Albuquerque, New Mexico, USA, pp. 299-304, 2011.

[79] J.-C. Latombe, *Robot Motion Planning*, Kluwer Academic Publishers, 1991.

[80] J.-P. Laumond, P. E. Jacobs, M. Taix, and R. M. Murray, "A Motion Planner for Nonholonomic Mobile Robots," *IEEE Transaction on Robotics and Automation,* vol. 10, pp. 577-593, 1994.

[81] B. Jung and G. S. Sukhatme, "Cooperative Multi-robot Target Tracking," in *The 8th International Symposium on Distributed Autonomous Robotic Systems*, Minneapolis, Minnesota, USA, pp. 81-90, 2006.

[82] M. Zoghi and M. H. Kahaei, "Adaptive sensor selection in wireless-sensor networks for target tracking," *IET Signal Processing,* vol. 4, pp. 530-536, 2010.

[83] L. M. Kaplan, "Global node selection for target localization in a distributed network of bearings-only sensors," *IEEE Transaction on Aerospace and Electronic Systems,* vol. 42, 2006.

[84] R. J. Kelly, "Reducing geometric dilution of precision using ridge regression signal processing," in *IEEE Conference on Position Location and Navigation Symposium*, Orlando, FL, pp. 461-469, 1988.

[85] R. Yarlagadda, I. Ali, N. Al-Dhahir, and J. Hershey, "GPS GDOP mtric," *IEE Proceedings on Radar, Sonar and Navigation,* vol. 147, 2000.

[86] M. Kalandros and L. Y. Pao, "Covariance Control for Multisensor Systems," *IEEE Transaction on Aerospace and Electronic Systems,* vol. 38, 2002.

[87] G. K. Atia, V. V. Veeravalli, and J. A. Fuemmeler, "Sensor Scheduling for Energy-Efficient Target Tracking in Sensor Networks," *IEEE Transaction on Signal Processing,* vol.59, no 10, pp.4923-4937, 2011.

[88] P. Pham and S. Commuri, "Stability and Perfomance of Wireless Sensor Networks during the Tracking of Dynamic Targets," in *Lecture Notes in Electrical Engineering*. vol. 89, J. Andrade Cetto, J.-L. Ferrier, and J. Filipe, Eds., ed, pp. 349-362, 2011.

[89] C. Chiang, H. Wu, W. Liu, and M. Gerla, "Routing In Clustered Multihop, Mobile Wireless Networks With Fading Channel," in *In Proc. IEEE SICON'97*, pp. 197-211, 1997.

[90] M. Boutayeb, H. Rafaralahy, and M. Darouach, "Covergence analysis of the Extended Kalman Filter as an observer for non-linear discrete-time systems," in *The 34th Conference on Decision and Control*, New Orleans, LA, pp. 1555-1560, 1995.

[91] Y. Bar-Shalom, X. R. Li, and T. Kirubarajan, *Estimation with Application to tracking and Navigation*, Wiley-Interscience, 2001.

[92] H. K. Khalil, *Nonlinear Systems*, Third ed.: Prentice Hall, 2001.

[93] S. Aeron, V. Saligrama, and D. A. Castañón, "Efficient Sensor Management Policies for Distributed Target Tracking in Multihop Sensor Networks," *IEEE Transaction on Signal Processing,* vol. 56, pp. 2562 - 2574, 2008.

[94] P. M. Djuric, M. Vemula, and M. F. Bugallo, "Target Tracking by Particle Filtering in Binary Sensor Networks " *IEEE Transaction on Signal Processing,* vol. 56, pp. 2229 - 2238, 2008.

[95] L. M. Kaplan, "Local node selection for localization in a distributed sensor network," *IEEE Transaction on Aerospace and Electronic Systems,* vol. 42, pp. 136-146, 2006.

[96] J. Lin, W. Xiao, F. L. Lewis, and L. Xie, "Energy-Efficient Distributed Adaptive Multisensor Scheduling for Target Tracking in Wireless Sensor Networks," *IEEE Transaction on Instrumentation and Measurement,* vol. 58, pp. 1886 - 1896 2009.

[97] J. A. Reeds and R. A. Shepp, "Optimal paths for a car that goes both forward and backwards," *Pacific Journal of Mathematics,* vol. 145, pp. 367-393, 1990.

[98] F. Zhao, J. Shin, and J. Reich, "Information-driven dynamic Sensor Collaboration," *IEEE Signal Processing Magazine,* vol. 19, pp. 61-72, 2002.

[99] J. Fang and H. Li, *IEEE Transaction on Wireless Communications,* vol. 8, pp. 3822 - 3832, 2009.

[100] S. Cui, J.-J. Xiao, A. Goldsmith, Z.-Q. Luo, and V. Poor, " Estimation Diversity and Energy Efficiency in Distributed Sensing " *IEEE Transaction on Signal Processing,* vol. 55, pp. 4683 - 4695, 2007.

[101] J. Lin, W. Xiao, F. Lewis, and L. Xie, "Energy-Efficient Distributed Adaptive Multisensor for Scheduling for Target Tracking in Wireless Sensor Networks," *IEEE Transaction on Instrumentation and Measurement,* vol. 58, pp. 1886 - 1896, 2009.

[102] S. Pattem, S. Poduri, and B. Krishnamachari, "Energy-quality tradeoffs for target tracking in wireless sensor networks," in *IPSN'03 Proceedings of the 2nd international conference on Information processing in sensor networks* Palo Alto, CA, pp. 32-46, 2003.

[103] J. A. Fuemmeler, G. K. Atia, and V. V. Veeravalli, "Sleep Control for Tracking in Sensor Networks," *IEEE Transaction on Signal Processing,* vol. 59, pp. 4354-4366, 2011.